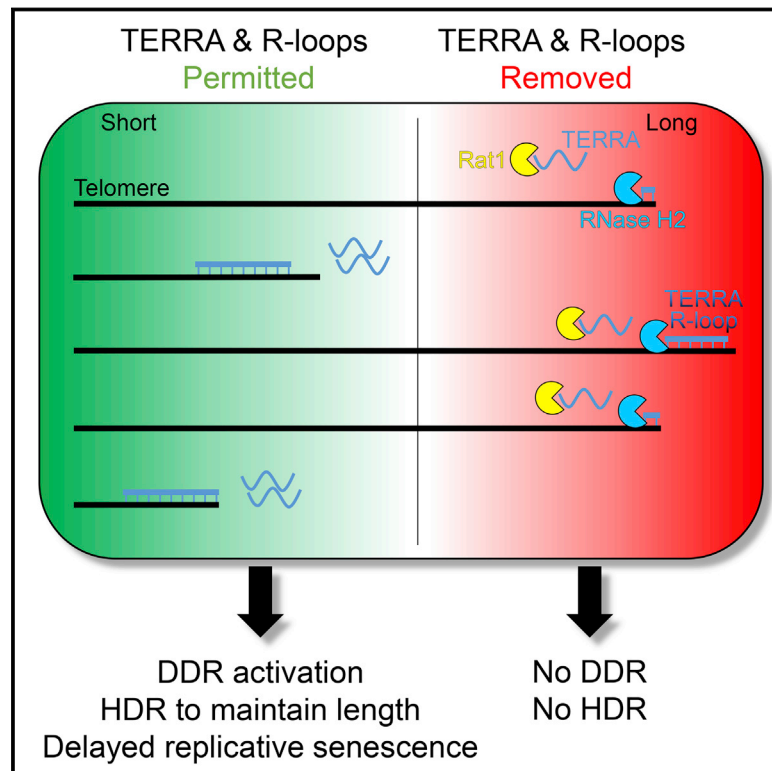# Telomere Length Determines TERRA and R-Loop Regulation through the Cell Cycle

Graphical Abstract

Authors

Marco Graf, Diego Bonetti, Arianna Lockhart, ..., Pascale Jolivet, Maria Teresa Teixeira, Brian Luke

Correspondence

b.luke@imb-mainz.de

In Brief

TERRA balances repair mechanisms at short telomeres to preserve genome integrity.

Highlights

- Rif2 recruits RNase H2 and Rat1 specifically to long telomeres

- At long telomeres, TERRA and R-loops are degraded prior to telomere replication

- TERRA and R-loops accumulate as telomeres shorten and activate the DDR

- TERRA R-loops promote homology-directed repair to avoid premature senescence

CellPress

Telomere Length Determines TERRA and R-Loop Regulation through the Cell Cycle

Marco Graf,[1,5] Diego Bonetti,[1,5,6] Arianna Lockhart,[1,5] Kamar Serhal,[3] Vanessa Kellner,[1] André Maicher,[4] Pascale Jolivet,[3] Maria Teresa Teixeira,[3] and Brian Luke[1,2,7,*]

[1]Institute of Molecular Biology (IMB), 55128 Mainz, Germany
[2]Faculty of Biology, Institute of Developmental Biology and Neurobiology, Johannes Gutenberg University Mainz, 55099 Mainz, Germany
[3]Institut de Biologie Physico-Chimique, UMR8226, Laboratoire de Biologie Moléculaire et Cellulaire des Eucaryotes CNRS, Sorbonne Universités, UPMC, Univ Paris 06, 75005 Paris, France
[4]Department of Molecular Microbiology and Biotechnology, Tel Aviv University, 69978 Tel Aviv, Israel
[5]These authors contributed equally
[6]Present address: Dipartimento di Biotecnologie e Bioscienze, Università degli Studi di Milano Bicocca, 20126 Milano, Italy
[7]Lead Contact
*Correspondence: b.luke@imb-mainz.de
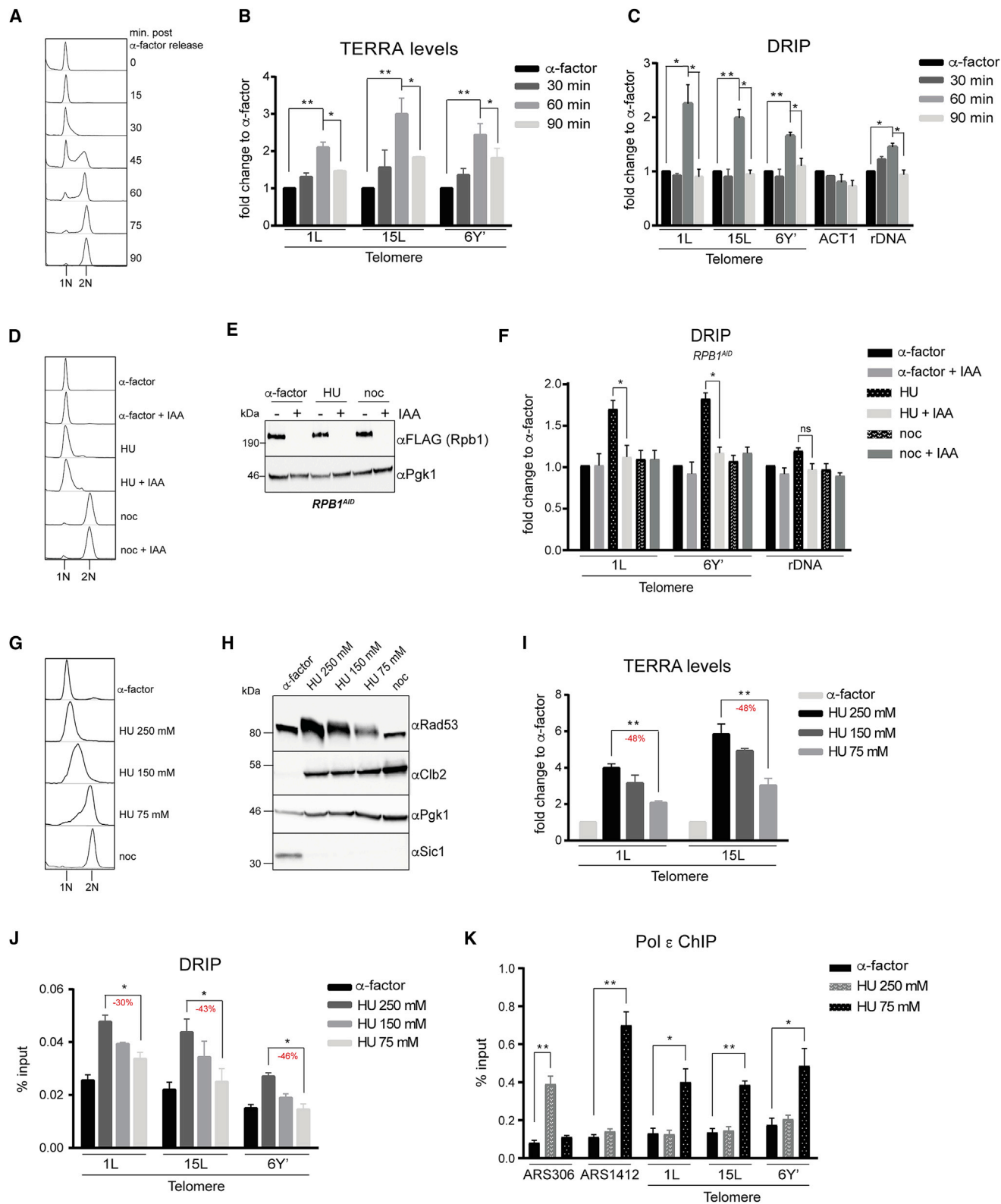http://dx.doi.org/10.1016/j.cell.2017.06.006

SUMMARY

Maintenance of a minimal telomere length is essential to prevent cellular senescence. When critically short telomeres arise in the absence of telomerase, they can be repaired by homology-directed repair (HDR) to prevent premature senescence onset. It is unclear why specifically the shortest telomeres are targeted for HDR. We demonstrate that the non-coding RNA TERRA accumulates as HDR-promoting RNA-DNA hybrids (R-loops) preferentially at very short telomeres. The increased level of TERRA and R-loops, exclusively at short telomeres, is due to a local defect in RNA degradation by the Rat1 and RNase H2 nucleases, respectively. Consequently, the coordination of TERRA degradation with telomere replication is altered at shortened telomeres. R-loop persistence at short telomeres contributes to activation of the DNA damage response (DDR) and promotes recruitment of the Rad51 recombinase. Thus, the telomere length-dependent regulation of TERRA and TERRA R-loops is a critical determinant of the rate of replicative senescence.

INTRODUCTION

Telomeres are nucleoprotein complexes harboring G-rich repetitive sequences that prevent repair activities at chromosome termini (Arnoult and Karlseder, 2015; de Lange, 2009). As the canonical replication machinery is unable to compensate for the end replication problem (Lingner et al., 1995; Soudet et al., 2014), telomeres shorten upon each passage through S phase. Telomerase, a reverse-transcriptase, counteracts telomere loss by adding de novo repeats to the 3′ ends (Greider and Blackburn, 1987; Hug and Lingner, 2006). Lack of telomerase activity leads to progressive telomere shortening, ultimately resulting in a permanent checkpoint-mediated arrest, referred to as replicative senescence (Campisi and d'Adda di Fagagna,

2007). In some metazoans, where telomerase becomes downregulated in somatic cells, replicative senescence is considered tumor-suppressive by limiting the number of divisions a proliferative cell can undergo. Telomere shortening must, however, be tightly regulated to ensure that senescence does not occur prematurely, which could lead to failed tissue regeneration potential. In yeast, one critically short telomere is sufficient to trigger senescence (Abdallah et al., 2009; Bourgeron et al., 2015; Xu et al., 2013), whereas four to five critically short telomeres are required in human cells (Kaul et al., 2011). At critically short telomeres, homology-directed repair (HDR) between sister chromatids can partially compensate for the loss of telomeric repeats in the absence of telomerase, thereby buffering against early onset senescence (Fallet et al., 2014). The in vivo activity of budding yeast telomerase requires the proteins Est1, Est2, Est3, and the RNA moiety TLC1 (Hughes et al., 1997). Deletion of any of these components results in replicative senescence following multiple population doublings (Abdallah et al., 2009; Hughes et al., 1997; Lundblad and Szostak, 1989) in a similar manner to human somatic cells where telomerase is not expressed (Teixeira, 2013). Yeast telomeres are bound by the Rap1 protein, which additionally recruits Rif1 and Rif2 (Hardy et al., 1992; Wotton and Shore, 1997) to promote end protection (Bonetti et al., 2010) and regulate the frequency of telomerase action (Teixeira et al., 2004). Rap1 also interacts with Sir3 and Sir4 that, together with the histone deacetylase Sir2, initiate heterochromatin formation in subtelomeric regions (Moretti et al., 1994). The distribution of Rif1 and Rif2 along telomere repeats may not be equal, and it has been suggested that Rif2 is enriched at the distal tip of the chromosome end, whereas Rif1 remains centromere proximal (McGee et al., 2010). Indeed, the loss of Rif2 precedes the loss of Rif1 during telomere shortening (McGee et al., 2010).

Telomeric repeat-containing RNA (TERRA) is transcribed at telomeres in a conserved manner from yeast to humans (Azzalin et al., 2007; Feuerhahn et al., 2010; Luke et al., 2008). TERRA is an RNA polymerase II (RNAPII) transcript that harbors sequence elements from the subtelomere and telomeric repeats (Luke et al., 2008). In yeast, TERRA levels are kept low by Rat1, a nuclear 5′-3′ RNA exonuclease (Luke et al., 2008). The

Sir2/Sir3/Sir4 complex also restricts TERRA expression, presumably via transcriptional repression (Iglesias et al., 2011). Rif1 and Rif2 additionally contribute to TERRA repression and genetic interactions suggest that this is Rat1-mediated (Iglesias et al., 2011). In human cells, TERRA levels and localization are cell-cycle regulated but its localization is perturbed in cancer cell lines that employ the alternative lengthening of telomeres (ALT) mechanism of telomere maintenance (Flynn et al., 2015; Porro et al., 2010). The nature of TERRA's cell-cycle regulation remains to be clarified.

It has been proposed that TERRA forms physiologically relevant RNA-DNA hybrids at telomeres (Arora and Azzalin, 2015; Balk et al., 2013; Rippe and Luke, 2015; Sagie et al., 2017). In human ALT cancer cell lines, as well as in the yeast equivalents (type II survivors), both TERRA levels and RNA-DNA hybrid abundance at telomeres are upregulated (Arora et al., 2014; Yu et al., 2014). Moreover, when telomeres become short during replicative senescence, TERRA abundance increases (Cusanelli et al., 2013; Moravec et al., 2016). RNA-DNA hybrids formed in a transcription-dependent manner are referred to as R-loops and lead to three-stranded nucleic acid structures, whereby the hybrid results in the displacement of one strand of DNA (Aguilera and García-Muse, 2012). When not resolved, R-loops pose a threat to genome stability by causing replication fork stalling and may trigger the formation of double-stranded breaks (DSBs) (Aguilera and Gómez-González, 2008; Houlard et al., 2011; Sollier and Cimprich, 2015). In yeast, there are multiple measures in place to protect the genome from RNA-DNA hybrid accumulation. Among these are the RNase H1 and H2 enzymes, which digest the RNA moiety of the hybrid (Cerritelli and Crouch, 2009), helicases like Sen1 and Pif1 that preferentially unwind hybrid molecules (Boulé and Zakian, 2007; Kim et al., 1999), and the THO-TREX complex that facilitates nuclear export of RNAs in a co-transcriptional manner (Huertas and Aguilera, 2003; Rondón et al., 2010).

RNA-DNA hybrids accumulate at yeast telomeres following the ablation of RNase H activity (Balk et al., 2013; Pfeiffer et al., 2013; Pfeiffer and Lingner, 2012). In telomerase-negative yeast, the elevated presence of RNA-DNA hybrids correlates with increased rates of HDR at telomeres and hence a delayed onset of replicative senescence (Balk et al., 2013). Interestingly, short telomeres are particularly prone to processing and eventual HDR in pre-senescent cells in order to prevent premature senescence (Fallet et al., 2014). It has been suggested that TERRA may be involved in forming R-loops at critically short telomeres to promote HDR (Balk et al., 2013; Rippe and Luke, 2015).

We demonstrate that critically short telomeres accumulate TERRA and TERRA R-loops, the latter of which are important to ensure that activation of the DNA damage response (DDR) occurs and prevents early senescence onset. We have elucidated the molecular mechanisms underlying this regulation. Our data indicate that the inability of cells to remove TERRA R-loops at critically short telomeres helps to ensure a *cis* regulatory mechanism to promote HDR specifically at short, and not long, telomeres, to prevent premature senescence.

RESULTS

TERRA and R-Loops Are Cell-Cycle Regulated

To understand how TERRA regulation and function are related, we measured its levels by qRT-PCR after releasing G1-arrested cells into the cell cycle (Figures 1A and 1B). TERRA levels peaked 60 min post-release (Figure 1B), corresponding to the S phase (Figure 1A). In agreement, TERRA levels increased in hydroxyurea (HU)-arrested cells (S phase), as compared to both α-factor (G1) and nocodazole (G2/M)-treated samples (Figures S1A and S1B). We used the S9.6 monoclonal antibody, which recognizes RNA-DNA hybrids of at least 6–8 bp (Phillips et al., 2013), to perform DNA-RNA immunoprecipitation (DRIP) on these synchronized samples. Similar to TERRA levels, RNA-DNA hybrids accumulate at telomeres 60 min post G1-release (Figure 1C) and in HU-arrested cells (Figure S1C). The DRIP signal was abolished following treatment with RNase H, demonstrating antibody specificity (Figure S1D).

We created an auxin-inducible degron (AID) version of the largest RNAPII subunit, Rpb1 ($RPB1^{AID}$), to rapidly degrade RNAPII and extinguish TERRA transcription upon the addition of auxin (indole-3-acetic acid [IAA]) (Morawska and Ulrich, 2013; Figures 1D and 1E). The increase of telomeric RNA-DNA hybrids (Figure 1F) as well as TERRA levels (Figure S1E) was abolished upon RNAPII degradation in S phase-arrested cells. We failed to detect an S phase-specific increase in telomeric RNA-DNA hybrids at modified telomere 7L* (Figure S1F), which

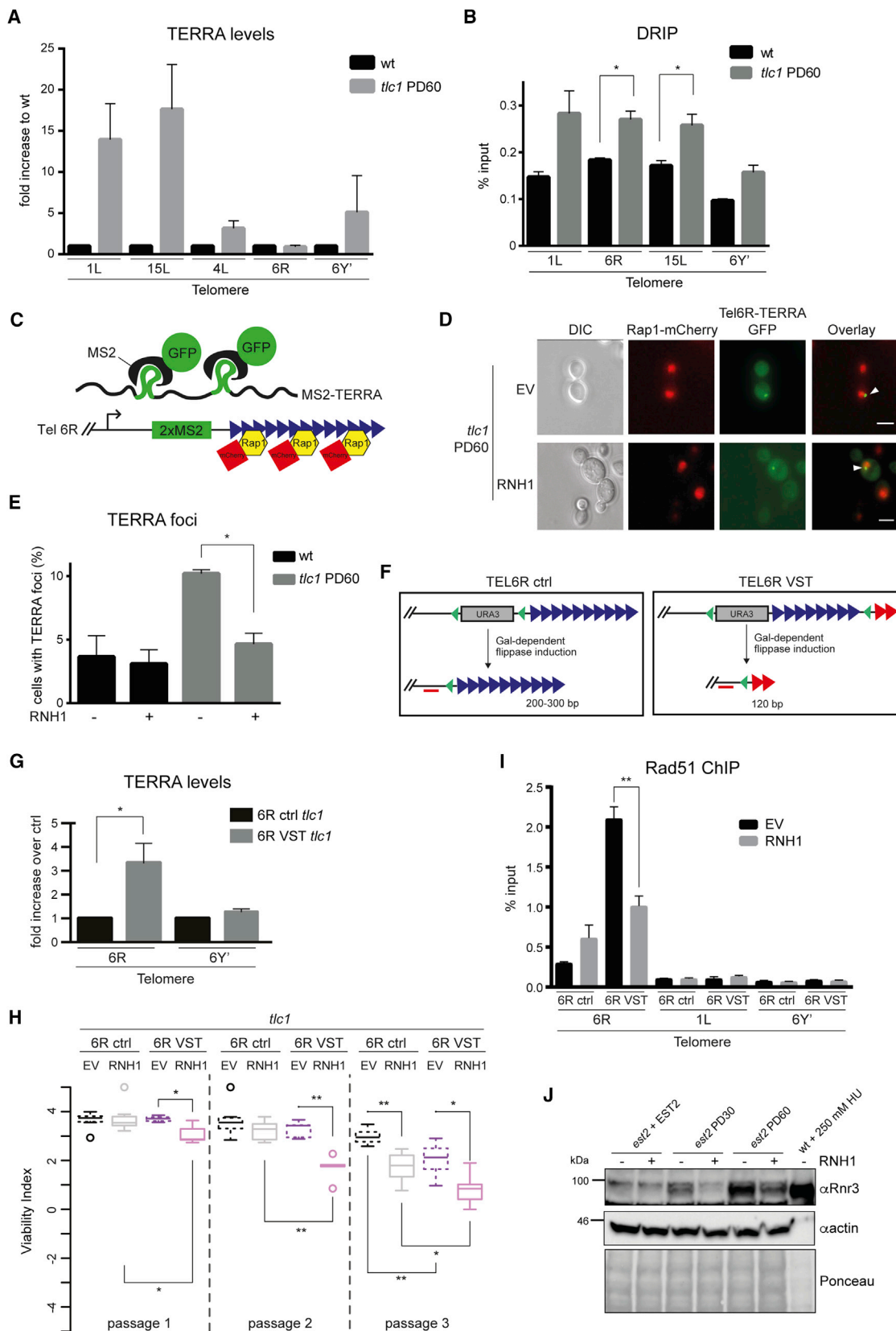**Figure 1. TERRA and TERRA R-Loops Decrease throughout the S Phase**

(A–C) Wild-type cells were synchronized in G1 with α-factor for 2 hr and released at 25°C. Samples were taken at the indicated time points for DNA content analysis by fluorescence-activated cell sorting (FACS) (A), RNA extraction (B), and DRIP (C). (B) Total RNA was reverse transcribed and TERRA from specific telomeres (1L, 15L, and 6Y') was analyzed by qPCR. Values are represented as % of *ACT1* RNA and relative to cells arrested in G1 that is set to 1 for each amplicon. (C) DRIP. Chromatin was immunoprecipitated using the S9.6 antibody and analyzed by qPCR at the indicated loci. Values are represented as % input of DNA recovered and relative to cells arrested in G1.

(D–F) Cells carrying an AID variant of the large subunit of the RNA polymerase II ($RPB1^{AID}$) were synchronized in G1, in S phase (200 mM HU), and at G2/M with 15 μg/mL nocodazole. IAA was added to half of the culture to 500 μM for 1 hr to deplete Rpb1. (D) DNA content was measured by FACS. (E) Rpb1 protein levels were analyzed before and after IAA addition using anti-FLAG antibodies. Pgk1 serves as a loading control. (F) DRIP was performed as in (C).

(G–J) Wild-type cells were synchronized in G1 and released at 30°C in the presence of the indicated concentrations of HU or 15 μg/mL nocodazole for 2 hr. (G) DNA content was measured by FACS. (H) Sic1 and Clb2 protein levels, as well as Rad53 phosphorylation were analyzed by western blot. (I) TERRA levels were analyzed as in (B). (J) DRIP was performed as in (C), but values are represented as % input of telomeric DNA recovered.

(K) Functional Pol2-9myc was immunoprecipitated from cross-linked extracts from cells arrested in G1 or released from G1 into 250 mM or 75 mM HU. Enrichment of telomeric DNA as well as early (ARS306) and a late (ARS1412) origins of replication were analyzed by qPCR. All data (A–K) are depicted as mean + SEM, n = 3. p values were obtained from two-tailed Student's t tests (*p < 0.05, **p < 0.01, ***p < 0.001).

See also Figure S1.

A TERRA levels

B DRIP

C

D Tel6R-TERRA

E TERRA foci

F TEL6R ctrl / TEL6R VST

G TERRA levels

H *tlc1*

I Rad51 ChIP

J

(legend on next page)

is defective for TERRA production (Balk et al., 2013), whereas other telomeres in the same strain accumulated RNA-DNA hybrids in the S phase.

TERRA and R-Loops Are Regulated within S Phase

Although the S phase in *S. cerevisiae* is short, it can be segmented using varying HU concentrations (Clarke et al., 2001). When G1-arrested cells are released into different concentrations of HU, we detect varying amounts of replication (Figure 1G) and Sic1 degradation, indicating passage through "Start" at the G1/S transition (Figure 1H). TERRA and R-loops accumulate when cells are released into high concentrations of HU (250 mM corresponding to limited replication) (Figures 1I and 1J) and decrease as genome duplication progresses (75 mM HU). The intra-S phase regulation of R-loops may be telomere-specific, as we did not observe similar trends when analyzing R-loops at either the actin or rDNA loci (Figure S1G). To define high (250 mM) versus low (75 mM) HU in terms of replication timing, we performed chromatin immunoprecipitation (ChIP) experiments with an epitope tagged version of DNA Polε. In cells arrested with 250 mM HU, we enriched DNA Polε at an early (ARS306) but not at a late (ARS1412) origin or at telomeres (Figure 1K). In contrast, DNA Polε could be found associated with telomeres and late, but not early, origins in the presence of 75 mM HU. Therefore, the decrease in TERRA levels/R-loops coincides with an increase in DNA Polε occupancy at telomeres, indicating TERRA intermediates are eliminated at the time of telomere replication.

To rule out that TERRA accumulation is a consequence of HU treatment (and checkpoint activation), we released replication defective *cdc7-4* cells from G1 at the restrictive temperature, resulting in early replication arrest without the corresponding checkpoint activation (Figure S1H). Similar to HU treatment, TERRA levels increase in early S phase (Figure S1I). This confirmed that the TERRA accumulation, which occurs at the G1/S transition, precedes the passage of the replication fork through the telomere. In addition, we observed an increase in TERRA in HU 250 mM-treated cells when the checkpoint was abolished (in *rad53* and *mec1* mutants, not shown).
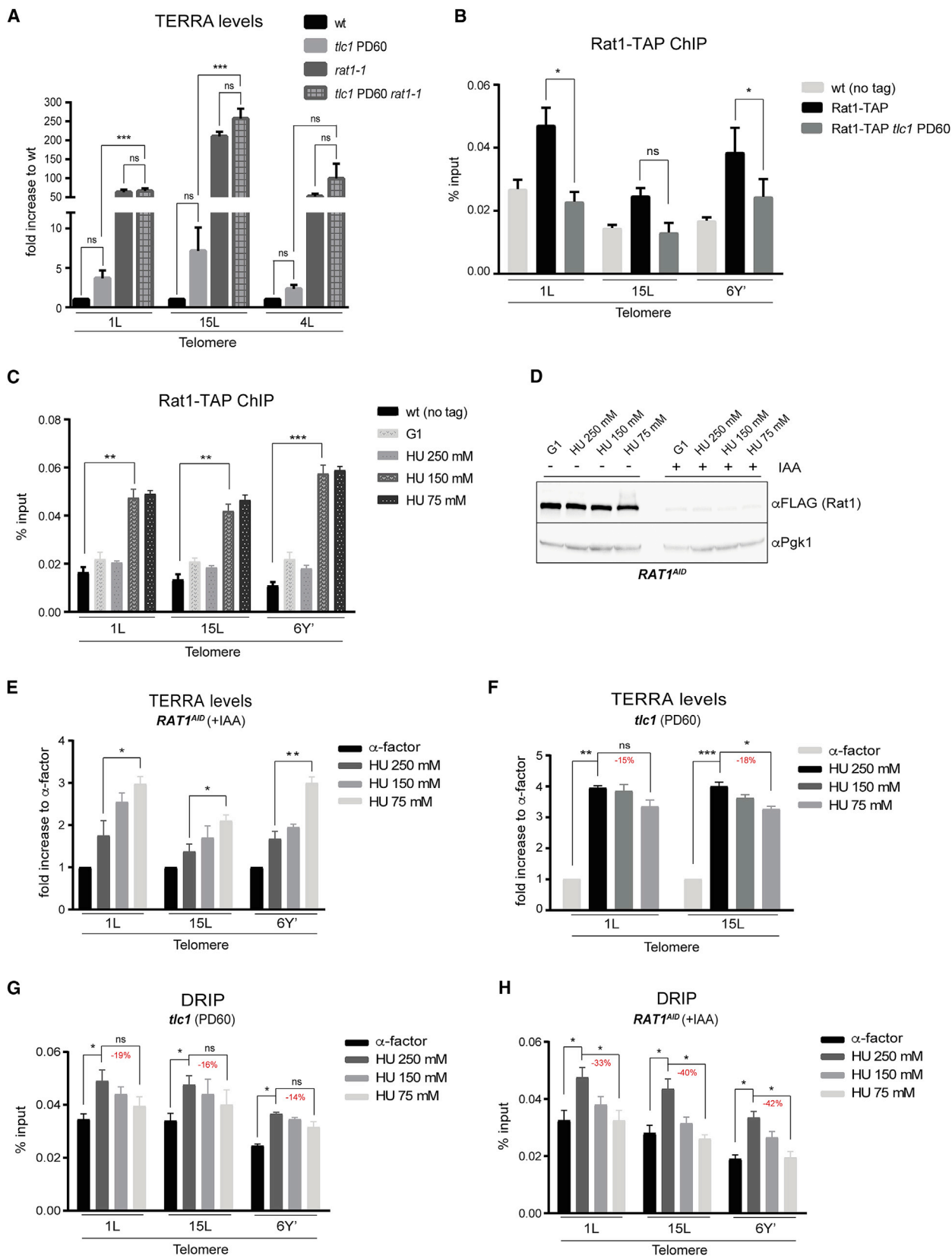
Critically Short Telomeres Accumulate TERRA R-Loops

To test whether R-loops also accumulate at short telomeres, we derived telomerase negative cells (*tlc1*) and allowed them to proliferate for 60 population doublings (PD60). *tlc1* PD60 cells had short telomeres but had not yet formed recombination-dependent survivors (Figure S2A). TERRA levels (Figure 2A) and RNA-DNA hybrid abundance (Figure 2B) increased at telomeres in *tlc1* PD60 cells. Although TERRA levels were reproducibly upregulated in pre-senescent cells, inter-clonal differences with regards to which telomeres upregulated TERRA as well as the fold change observed varied, suggesting the involvement of a stochastic event.

To determine if the increased TERRA/R-loop levels was due to the altered cell-cycle distribution of pre-senescent cells, wild-type and *tlc1* PD60 cells were synchronized at the G2/M border with nocodazole (Figure S2B), and total TERRA levels were evaluated (Figure S2C). Even in synchronous cultures, TERRA levels were increased in *tlc1* mutants with short telomeres as compared to wild-type cells. To assign the increase of RNA-DNA hybrid levels at short telomeres to TERRA, we employed a fluorescence microscopy-based assay to detect endogenous TERRA molecules generated from a single telomere (Cusanelli et al., 2013). In these cells, the TERRA locus at telomere 6R (Tel6R) harbors MS2 stem loops 80 bp upstream of the telomeric repeats, which can be visualized by expressing an MS2-GFP fusion. The nucleoplasm and telomeric clusters were marked by a Rap1-mCherry fusion protein (Figure 2C). We quantified those TERRA foci that were adjacent or overlapping with Rap1-mCherry signals and detected a 2-fold increase in nuclear TERRA foci in pre-senescent, compared to wild-type cells (Figures 2D and 2E) in agreement with published results (Cusanelli et al., 2013). Upon overexpression of *RNH1*, to degrade

---

Figure 2. The DDR at Shortened Telomeres Requires the Presence of R-Loops

(A) TERRA levels were measured as in Figure 1. TERRA values were normalized to the respective actin value and levels in *tlc1* PD60 were normalized to the respective wild-type (WT). The mean values + SEM are displayed, n = 3.

(B) DRIP was performed in pre-senescent cells. Enrichment was measured via qPCR and mean values compared to the respective input + SEM are shown, n = 3 (*p < 0.05).

(C) Schematic representation of the Tel6R-TERRA-MS2-GFP. Blue arrowheads represent telomeric repeats and the black arrow depicts the approximate TERRA transcription start site.

(D) Live-cell microscopy analysis of Tel6R-TERRA-GFP foci in cells of the indicated genotypes containing an empty vector (EV) or overexpressing Rnh1 (RNH1). Nuclei and telomeric clusters were identified by visualizing Rap1-mCherry foci. Representative images of *tlc1* cells are shown. Scale bar, 5 μm.

(E) Quantification of cells containing a Tel6R-TERRA-GFP focus adjacent or overlapping with Rap1-mCherry signals. Data are shown as mean + SEM of two independent experiments in which 300 cells were counted. A ratio paired two-tailed Student's t test was performed (*p < 0.05).

(F) Schematic of the generation of a very short telomere (VST) 6R. Triangles, FRT site (green), telomeric repeats (blue), telomeric repeats of the VST (red); red line, site of the amplicon for qPCR.

(G) TERRA levels were measured as in (A). Error bars represent SEM, n = 6 (*p < 0.05, unpaired Student's t test).

(H) After the flip-out, eight independent spores of each genotype were spotted in serial dilutions onto SD plates (passage I) and grown cells were subjected to serial passages (passage II and III). Viability was quantified by measuring the pixel intensity of each spot via ImageJ and by comparing it to a *TLC1* control as described (Fallet et al., 2014). Adjusted p values were obtained by Wilcoxon rank-sum test with a false discovery rate correction *p < 0.1 and **p < 0.05. 6R ctrl EV n = 8; 6R ctrl RNH1 n = 8; 6R VST EV n =5; 6R VST RNH1 n = 5. See Table S3 for detailed p values.

(I) Rad51 recruitment to the shortest telomere is RNA-DNA hybrid-dependent. Cross-linked samples of indicated strains were subjected to anti-Rad51 ChIP. Enrichment of particular loci were determined via qPCR. The mean % input values are displayed as + SEM, n = 3 (**p < 0.01).

(J) Senescent *est2* cells were transformed with an inducible *RNH1* expression vector. *RNH1* was induced 3 hr prior to protein extraction, which was subjected to western blotting with anti-Rnr3 antibodies. Only 10% are loaded for WT + HU.

See also Figure S2.

(legend on next page)

RNA-DNA hybrids, the percentage of pre-senescent cells with TERRA foci was reduced.

TERRA Promotes the DDR at Critically Short Telomeres

We hypothesized that a stochastic event, such as the generation of a critically short telomere, may account for the variability observed in terms of TERRA and TERRA hybrid upregulation during replicative senescence (Figures 2A and 2B). To address this, we adapted a previously described construct (Marcand et al., 1999) to generate one critically short telomere without disturbing the subtelomere, and hence TERRA regulatory sequences. We integrated a *URA3* cassette followed by telomeric repeats and flanked by the flippase recognition target sites (FRT sites) into the subtelomere of telomere 6R. When *FLP1* is induced, the *URA3* cassette together with a substantial amount of telomeric repeat DNA is "flipped out," leaving a very short telomere (VST) of 120 bp (Figures 2F, right panel, and S2D–S2G). A control strain (6R ctrl) results in the generation of a 200–300 bp telomere following the identical recombinase reaction (Figure 2F, left panel).

When 6R telomere shortening was induced in a *tlc1* background, TERRA and RNA-DNA hybrids at telomere 6R VST were increased compared to the control strain in a manner that was sensitive to RNase H1 overexpression (Figures 2G and S2H). In the same cells, the non-shortened telomeres (6Y′) did not upregulate TERRA or hybrids. This indicates that accumulation of TERRA and RNA-DNA hybrids in pre-senescent cells is a particular feature of critically short telomeres. We assayed senescence rates in 6R ctrl and 6R VST strains that harbored either an empty vector (EV) or an *RNH1* overexpression vector (RNH1) (Figure 2H). Replicate clones of the indicated strains were spotted in serial dilutions onto agar plates and passaged three times to accumulate population doublings. The 6R VST strain that overexpressed *RNH1* senesced faster than the 6R VST strains with vector control, already at passage 1, whereas increased *RNH1* expression only affected the control strain at passage 3. Importantly, the accumulation of Rad51 at the VST (Fallet et al., 2014) was reduced when *RNH1* expression was induced (Figure 2I). Moreover, the senescence-associated checkpoint response, as monitored by *RNR3* expression, was greatly diminished in *tlc1* cells upon *RNH1* overexpression (Figure 2J). In summary, these data are congruent with the notion that TERRA R-loops are critical to establish the DDR, and hence promote HDR

at critically shortened telomeres to prevent premature senescence.

Loss of Rat1 at Short Telomeres Accounts for Increased TERRA Levels, but Not R-Loops

Higher TERRA levels in pre-senescent cells could be due to either loss of Sir2 (Iglesias et al., 2011) or Rat1 function (Luke et al., 2008). If the loss of Sir2 function at short telomeres was responsible for TERRA increase, then an epistatic genetic interaction would be expected (i.e., the loss of Sir2 combined with shortened telomeres should not lead to a further increase in TERRA). Accordingly, we compared TERRA levels in *tlc1*, *sir2*, and *tlc1 sir2* mutants (Figure S3A). TERRA levels in *sir2* cells increased up to 100-fold compared to wild-type and up to 15-fold in pre-senescent *tlc1* cells. In *tlc1 sir2* cells, TERRA increased in an additive manner when compared to both single mutants, suggesting that the loss of Sir2-mediated silencing is not the cause of increased TERRA at short telomeres. Consistently, we did not detect less Sir2 protein at shortened telomeres by ChIP (Figure S3B). Moreover, neither total RNAPII nor the active elongating form (pS2-RNAPII) was increased at telomeres in pre-senescent compared to wild-type cells (Figures S3C–S3E). Additionally, RNA-DNA hybrid levels in *sir2* mutants are unchanged with respect to wild-type (Figure S3F).

TERRA levels in *rat1-1* mutant cells increased up to 200-fold compared to wild-type following a shift to the restrictive temperature of 37°C as described (Figure 3A; Iglesias et al., 2011; Luke et al., 2008) and were increased in *tlc1* cells up to 7-fold in this experiment. TERRA abundance in the double mutant *tlc1 rat1-1* was not additive in comparison to the *rat1-1* single mutant, thereby providing genetic evidence that loss of Rat1 function may be responsible for increased TERRA at shortened telomeres. Moreover, the ability to detect Rat1 at telomeres by ChIP was lost when telomeres were shortened (Figure 3B). The decreased association of Rat1 to short telomeres may be in part due to the decreased levels of the Rat1 protein in senescent, compared to non-senescent, cells (Figure S3G).

We tested whether the degradation of TERRA in late S phase (Figure 1I) may be Rat1-dependent. In support of this, Rat1 gets recruited to telomeres in 150 mM and 75 mM HU-arrested cells (Figure 3C), corresponding to late S phase when TERRA levels decrease and telomeres get replicated (see Figures 1I and 1K). The reduction of TERRA in late S phase was abrogated when Rat1 was inactivated using a degradable version (*RAT1^AID*)

Figure 3. Rat1 Controls TERRA Levels, but Not R-Loops, through the Cell Cycle

(A) Cells were grown to exponential phase and shifted to 37°C for 1 hr to inactivate Rat1. TERRA levels were measured as described.

(B) ChIP of crosslinked samples was performed at wild-type length and short telomeres. An untagged wild-type was used as a background control.

(C) Cells expressing a TAP-tagged Rat1 variant were synchronized in G1 and released in the presence HU for 2 hr. ChIP was performed and the enrichment of specific telomeric loci was analyzed. An untagged wild-type strain were used as a background control. Values are represented as % input of DNA recovered.

(D and E) Cells carrying an AID variant of the Rat1 protein (*RAT1^AID*) were synchronized in G1 and released in S phase in the presence of HU for 2 hr. IAA was added for 1 hr to half of the cultures, including G1 arrested cells, to 500 μM final concentration to induce Rat1 depletion. (D) Rat1 protein levels were analyzed using anti-FLAG antibodies. (E) TERRA levels were measured as in Figure 1B.

(F and G) *tlc1* cells were grown for approx. 60 PDs following dissection of a heterozygous diploid. Cells were synchronized in G1 and released in the presence of HU for 2 hr. (F) TERRA was measured as in Figure 1B. (G) DRIP analysis was performed on extracts derived from the same experiment as in (F). Values are represented as % input.

(H) DRIP was performed on extracts derived from the same experiment as in (D). All data are depicted as mean + SEM n = 3. p values were obtained from two-tailed Student's t tests (*p < 0.05, **p < 0.01, ***p < 0.001, ns, not significant).

See also Figure S3.
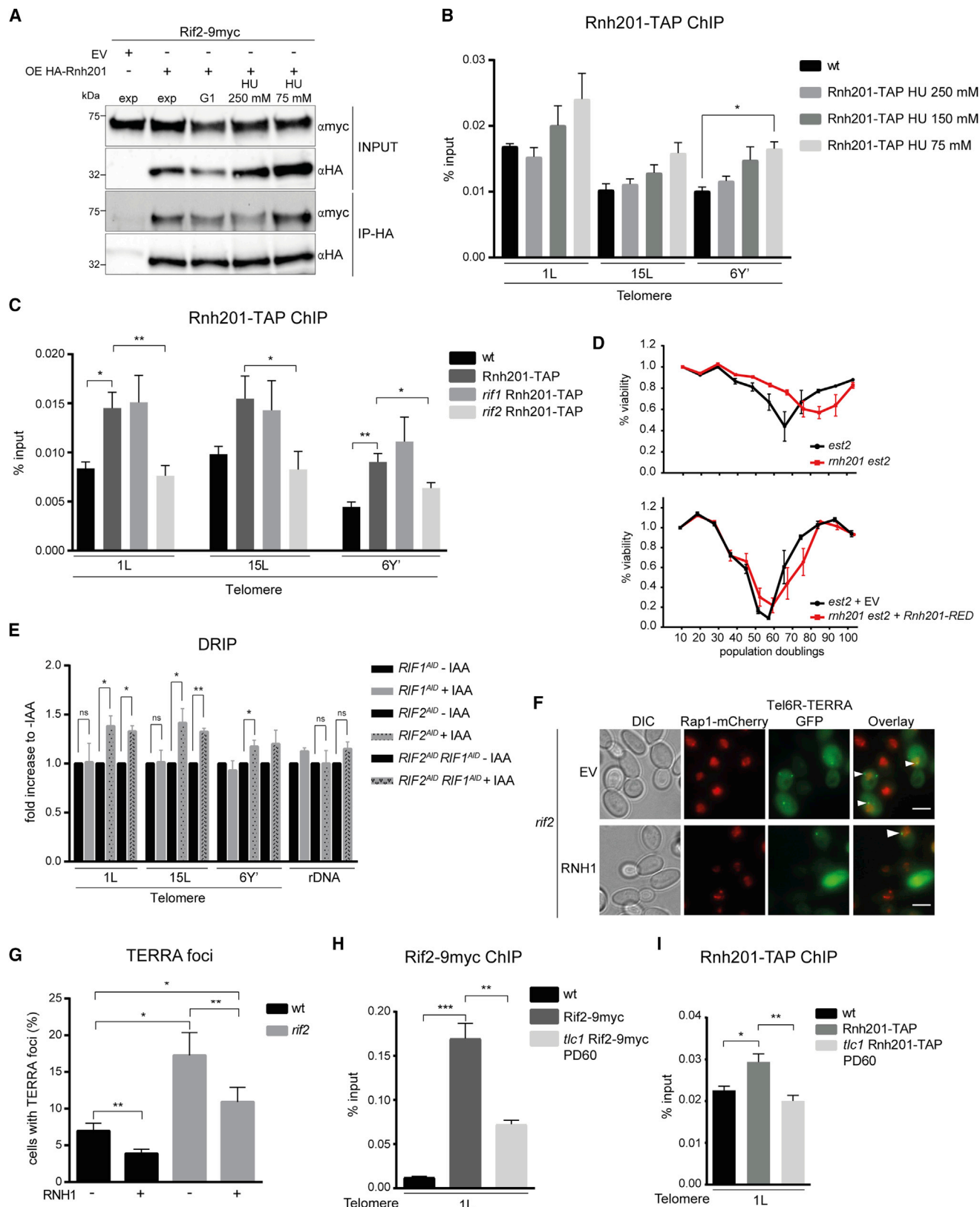
(legend on next page)

(Figures 3D and 3E). These results indicate that Rat1-mediated degradation of TERRA occurs approximately when telomeres get replicated.

Because shortened telomeres are associated with reduced amounts of Rat1, we predicted that the intra-S phase degradation of TERRA would be defective in pre-senescent cells. Indeed, we only detect a 15%–18% reduction in TERRA between early (250 mM HU) and late (75 mM HU) S phase, when telomeres are short (*tlc1* PD60) (Figure 3F), as compared to a 48% reduction in cells with normal length telomeres (Figure 1I). The removal of TERRA R-loops throughout the S phase was also defective at shortened telomeres. Whereas hybrids were decreased by 30%, 43%, and 46% at telomeres 1L, 15L, and 6Y′, respectively, in wild-type cells (Figure 1J), they were only reduced by 19%, 16%, and 14% in *tlc1* cultures with short telomeres (Figure 3G). In contrast to TERRA levels, TERRA R-loops were not stabilized upon Rat1 degradation with auxin (Figure 3H). Although the degradation through S phase is impaired, TERRA does eventually get degraded when cells with short telomeres exit the S phase and enter G2/M (Figure S3H).

In summary, TERRA levels are increased in pre-senescent cells due to the inability of short telomeres to associate with Rat1. As a consequence, TERRA degradation is hampered through the S phase in cells harboring shortened telomeres. The deregulation of R-loops at short telomeres appears to be unrelated to the loss of Rat1.

Rif2 Recruits RNase H2 to Long Telomeres to Limit TERRA R-Loops

RNase H1 and RNase H2 activities cooperate to restrict RNA-DNA hybrids at yeast telomeres (Balk et al., 2013; Pfeiffer et al., 2013). The catalytic subunit of RNase H2, Rnh201, was found to interact with the telomere-associated protein Rif2 in a yeast two-hybrid screen (Jeong et al., 2004). We attempted to co-immunoprecipitate (coIP) the two proteins from yeast whole cell extracts. An HA pull-down was performed in cells containing an empty vector (EV) or a plasmid overexpressing HA-tagged Rnh201 (HA-Rnh201) in the presence or absence of a functional

9myc-tagged Rif2 (Rif2-9myc) (Figure S4A). The pull-down of HA-Rnh201 led to the recovery of Rif2-9myc in the immunoprecipitated fraction (Figure 4A) from exponentially growing asynchronous cells. In synchronized cultures, the interaction between Rif2 and Rnh201 was increased in late, as compared to early, S phase, suggesting that Rnh201 may be recruited to telomeres when TERRA R-loops are removed (Figure 1J). ChIP experiments revealed that endogenously tagged Rnh201 (Rnh201-TAP) accumulates at telomeres as cells progress further into the S phase (75 mM HU) (Figures 4B and S4B), despite the fact that expression remains unchanged between early and late S phase (Figure S4C). We were also able to recover Rif1-9myc (Figure S4D), but not Rap1 (a Rif1 and Rif2 interacting factor, not shown), following the precipitation of Rnh201. Because Rif1 and Rif2 interact with Rnh201, we tested whether they were responsible for recruiting Rnh201 to telomeres. An endogenously expressed Rnh201-TAP-dependent ChIP signal could be detected above background (non-tagged wild-type cells) at all tested telomeres, however, the signal was lost when *RIF2,* but not *RIF1,* was deleted (Figure 4C). Rnh201-TAP protein levels were not altered upon deletion of either *RIF1* or *RIF2* (Figure S4E). We were unable to enrich endogenously expressed Rnh1 at telomeres by ChIP (Figure S4F) despite the fact that it can also interact with both Rif1 and Rif2 when overexpressed. The recruitment of Rat1 to telomeres was also dependent on the continued presence of both Rif1 and Rif2 (Figure S4G), consistent with genetic evidence demonstrating that increased TERRA levels in *rif1 rif2* mutants is not additive with the loss of Rat1 function (Iglesias et al., 2011). Together, these data indicate that RNase H2 is localized at telomeres in a Rif2-dependent manner and likely provides the majority of the RNase H activity at chromosome ends. RNase H2 has two discernable enzymatic activities, the removal of single misincorporated ribonucleotides from the DNA and the degradation of longer RNA-DNA hybrids, such as R-loops (Cerritelli and Crouch, 2009). We analyzed rates of senescence with telomerase negative cells in combination with loss of *RNH201* and complemented with the ribonucleotide excision defective (*RED*) allele

---

Figure 4. Rif2 Recruits RNase H Activity to Telomeres

(A) coIP of Rif2-9myc and overexpressed HA-Rnh201. Cells were either growing exponentially or synchronized with the indicated reagents for 2.5 hr. Immunoprecipitation (IP) was performed on protein extracts with anti-HA antibodies coupled magnetic beads, followed by immunoblotting with anti-HA or anti-MYC antibody, respectively. Input protein (2.5%) was loaded as control for immunoblotting. EV, empty vector.

(B) ChIP on cross-linked samples was performed to determine the abundance of TAP-tagged Rnh201 at telomeres at different stages of S phase. The mean values + SEM are depicted, n = 3 (*p < 0.05).

(C) ChIP assay using IgG coupled Sepharose on cross-linked samples from cells of the indicated genotypes was followed by qPCR. Values are represented as percent input of DNA recovered. Data are depicted as mean + SEM n = 3 for the WT, n = 6 for Rnh201-TAP, n = 6 for *rif1* Rnh201-TAP, and n = 4 for *rif2* Rnh201-TAP (*p < 0.05, **p < 0.01).

(D) Senescence curves were performed and viability was estimated daily by measuring cell culture density. Data are shown as mean ± SEM n = 5 per genotype.

(E) Cells carrying an AID of Rif1 (*RIF1^{AID}*), Rif2 (*RIF2^{AID}*), and their combination (*RIF1^{AID} RIF2^{AID}*) were grown to exponential phase. IAA was added to half of each culture to 500 μM for 3 hr (Figure S4I). DRIP analysis was performed as in Figure 1C, and values were plotted relative to the corresponding un-induced control which is set to 1 for each primer set. Data are represented as the mean + SEM, n = 4.

(F and G) *rif2* cells have increased amounts of 6R-TERRA nuclear foci. Live-cell microscopy analysis of Tel6R-TERRA-GFP foci in cells of the indicated genotypes containing empty vector (EV) or overexpressing Rnh1 (RNH1). Nuclei and telomeric clusters were identified by visualizing Rap1-mCherry foci. Representative images of *rif2* mutants are shown (F). Scale bar, 5 μm. (G) Quantification of cells containing a Tel6R-TERRA-GFP focus adjacent or overlapping with Rap1-mCherry signals. Data are shown as mean + SEM of two independent experiments in which at least 300 cells were counted. A ratio paired two-tailed Student's t test was performed (*p < 0.05, **p < 0.01).

(H and I) ChIP was performed on cells expressing a functional Rif2-9myc (H) or Rnh201-TAP (I) in both wild-type and *tlc1* cells that had undergone 60 PDs. Plots represent the mean + SEM, n = 5 (*p < 0.05, **p < 0.01, ***p < 0.001).

See also Figure S4.

of *RNH201* (Chon et al., 2013; Cornelio et al., 2017; Epshtein et al., 2016; Huang et al., 2017). Loss of *rnh201* led to a decreased rate of replicative senescence, in agreement with the notion that RNA-DNA hybrids promote HDR and prevent early senescence onset in yeast (Figure 4D) (Balk et al., 2013). The delay in replicative senescence was abolished upon expression of the *RNH201-RED* allele. These data are consistent with the notion that RNase H2 removes consecutive RNA-DNA hybrids from telomeres, such as TERRA R-loops.

rnh1 rnh201 double mutants are sensitive to the DNA damaging agent methyl methanesulphonate (MMS) (Lazzaro et al., 2012), however, *rnh1 rif2* mutants are not MMS-sensitive (Figure S4H), indicating Rif2 may specifically be required for RNase H2 function at telomeres.

TERRA R-Loops Accumulate in *rif2* Cells

Due to the interactions between the RNase H enzymes and Rif2, we speculated that R-loops may accumulate at telomeres in the absence of Rif2. We performed DRIP in wild-type, *RIF2^{AID}*, *RIF1^{AID}*, and *RIF1^{AID} RIF2^{AID}* cells following IAA induction to induce degradation (Figure S4I) and minimize telomere length effects associated with the deletion mutants. We observed that following the loss of Rif2, and not Rif1, an accumulation of hybrids was observed at all telomeres tested (Figure 4E). Loss of both Rif1 and Rif2 did not further increase the amount of R-loops at telomeres. Telomeric R-loops were also increased in *rif2* deletion cells, and this signal was reduced following the in vivo overexpression of RNase H1, confirming the specificity of the DRIP signal and indicating that RNase H1 can compensate for the loss of RNase H2 at telomeres, when overexpressed (Figure S4J).

There was an increase in the percentage of cells with TERRA-MS2-GFP foci that co-localize with Rap1 when *RIF2* is deleted in accordance with a previous study (Cusanelli et al., 2013). The percentage of cells with TERRA foci was reduced upon in vivo overexpression of RNase H1 in both wild-type and *rif2* cells (Figures 4F and 4G). These results substantiate the involvement of TERRA in RNA-DNA hybrids at telomeres and reveal that these hybrids accumulate in *rif2* cells. Finally, as telomeres shorten in the absence of telomerase, both Rif2 (McGee et al., 2010) and Rnh201 are lost from telomeres (Figures 4H and 4I). These data demonstrate that Rif2 regulates TERRA R-loop metabolism in terms of interacting with the RNase H2 enzyme and hence preventing R-loop formation at telomeres.

DISCUSSION

A myriad of studies indicate that R-loops play a physiologically relevant role at telomeres (Arora et al., 2014; Balk et al., 2013, 2014; Nanavaty et al., 2017; Pfeiffer et al., 2013; Pfeiffer and Lingner, 2012; Rippe and Luke, 2015; Sagie et al., 2017; Yu et al., 2014). This becomes apparent in pre- and post-senescent telomerase negative cells that employ HDR to maintain their telomeres. Post-senescent cancer cells using the ALT mechanism of telomere maintenance, as well as the yeast equivalents (type II survivors), depend on RNA-DNA hybrids at telomeres to promote proper elongation (Arora et al., 2014; Yu et al., 2014). In pre-senescent yeast, RNA-DNA hybrids promote HDR as telomeres shorten and delay senescence onset (Balk et al., 2013). A recent study has shown that the controlled regulation of R-loops at DNA double strand breaks ensures the proper formation of 3′ single-stranded DNA (ssDNA), a critical intermediate for the HDR reaction (Ohle et al., 2016). Here, we present data demonstrating that TERRA levels and TERRA R-loops are tightly regulated through the cell cycle. Upon telomere shortening, TERRA regulation is altered, resulting in the accumulation of TERRA levels and TERRA R-loops, the latter of which promote DDR activation and HDR at critically short telomeres to prevent premature senescence onset.

TERRA and TERRA R-loops are formed in the S phase of the cell cycle before DNA polymerase ε replicates telomeres (Figure 1). When telomeres are of a normal length, both TERRA levels and TERRA R-loops decline as DNA Pol ε arrives at telomeres. The decrease in TERRA levels through S phase is consistent with previous experiments performed in human cells (Flynn et al., 2015; Porro et al., 2010). We conclude that TERRA transcription precedes telomere replication, whereas the degradation of TERRA and R-loops occurs with approximately the same timing as DNA replication through the telomeric tract (Figure 5, step 1). The removal of TERRA and R-loops prior to the passage of the replisome may facilitate unperturbed replication progression at chromosome ends by preventing deleterious replication-transcription encounters (Aguilera and Gómez-González, 2008; Hamperl and Cimprich, 2016). Interestingly, replication stress occurs specifically on the leading strand (where TERRA R-loops form) when *UPF1* is depleted and TERRA accumulates at telomeres (Chawla et al., 2011).

The RNase H1 and H2 enzymes remove R-loops at telomeres (Arora et al., 2014; Balk et al., 2013; Pfeiffer et al., 2013; Pfeiffer and Lingner, 2012). Both RNase H enzymes can interact with the telomere bound factors, Rif1 and Rif2 (Figure 4), the latter of which recruits RNase H2 to telomeres. We were unable to detect RNase H1 at telomeres by ChIP, suggesting that RNase H2 may be primarily responsible for removing TERRA R-loops whereas RNase H1 plays an auxiliary/compensatory role. When telomeres are long, the recruitment of RNase H2 to telomeres, as well as its interaction with Rif2, occurs with similar timing to the removal of TERRA R-loops (in late S phase) thereby ensuring that R-loop removal and telomere replication are coordinated. When telomeres become critically short, Rif2 (McGee et al., 2010), and hence RNase H2, are lost at chromosomes ends (Figures 4 and 5, step 2). As a consequence, R-loops are less efficiently degraded (Figure 3G), and there is a greater chance that the oncoming replication machinery will encounter them in a co-directional manner (Figure 5, step 3). This probability is further increased due to the fact that short telomeres replicate earlier in the S phase than long telomeres (Bianchi and Shore, 2007). When the replication machinery encounters R-loops, it results in replication stress and DSB induction, which can trigger HDR (Aguilera and Gómez-González, 2008; Hamperl and Cimprich, 2016). At a critically shortened telomere, HDR promotes re-elongation and the avoidance of the critically shortened telomere to induce senescence (Figure 5, step 3). Indeed, the activation of the DDR and accumulation of Rad51 at critically short telomeres was abolished upon RNase H1
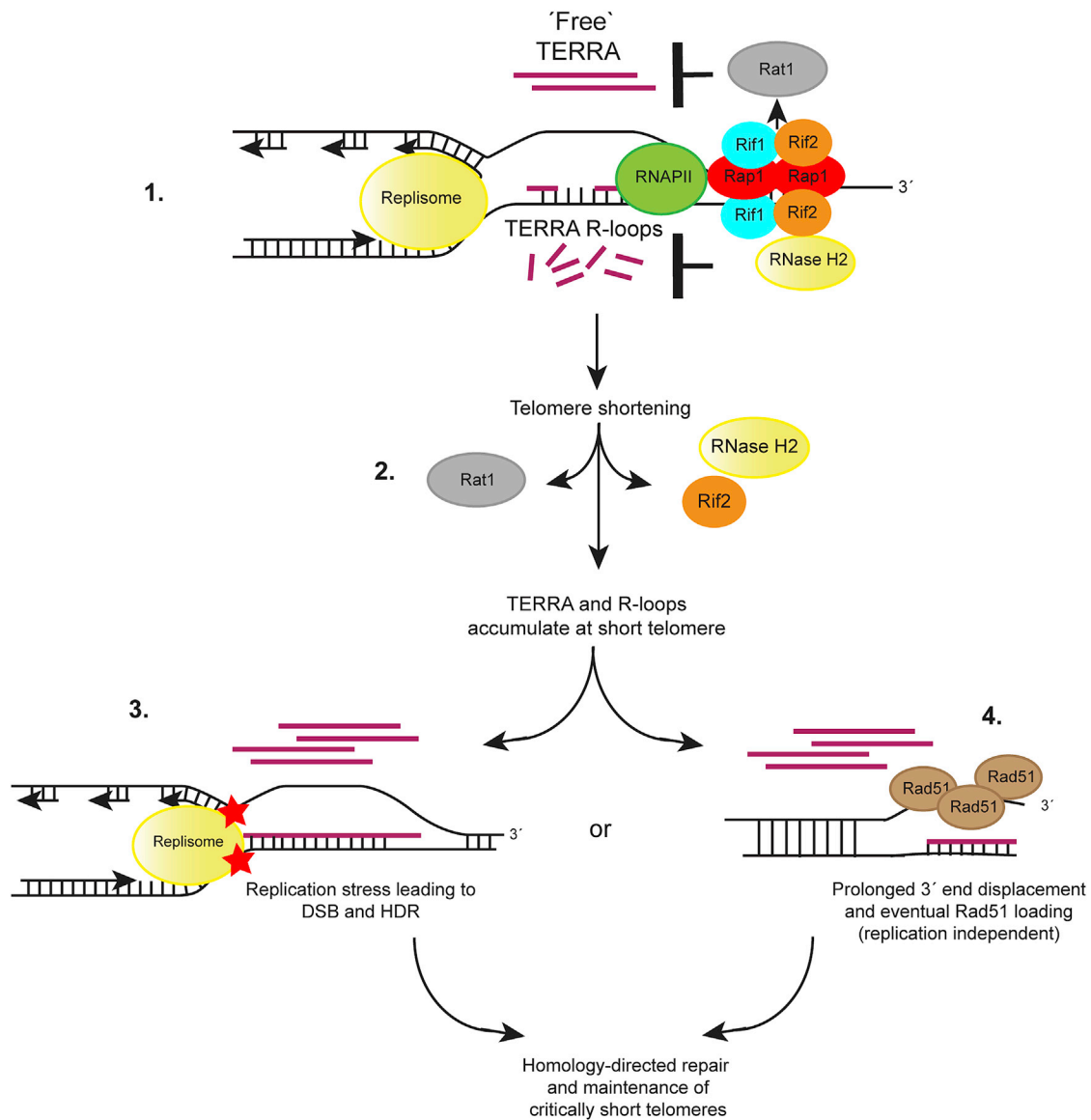
Figure 5. The Length-Dependent Regulation of TERRA Hybrids

At normal-length telomeres a sufficient number of Rif2-Rnh201 molecules can mediate an Rnh201-dependent degradation of TERRA-telomere hybrids. The exonuclease Rat1 that has been shown to genetically interact with Rap1 and Rif1 suppresses high TERRA levels through degradation, while the Sir2 deacetylase likely suppresses TERRA transcription (upper diagram). Upon telomere shortening, Rif2 is lost and hence Rnh201 is no longer recruited thereby allowing RNA-DNA hybrids to accumulate. Additionally, Rat1 appears to be less active toward TERRA degradation at short telomeres, thereby accounting for the increase in TERRA levels. TERRA inhibition via Sir2 remains intact at short telomeres. The accumulation of TERRA R-loops at short telomeres promotes DDR activation and HDR-mediated re-elongation to prevent premature senescence onset. Please see Discussion for a more detailed description.

overexpression, suggesting that R-loops are necessary for HDR to occur. This is likely conserved from yeast to humans, as short telomeres from human ICF (immunodeficiency, centromeric instability, and facial anomalies) syndrome cells also harbor increased TERRA R-loops, which leads to increased damaged signaling at chromosome ends (Sagie et al., 2017). Although the timing of events supports the above-described replication stress-dependent model of R-loop-induced HDR at telomeres (Figure 5, step 3), we cannot rule out other possibilities. The failure to remove TERRA R-loops may simply result in

the prolonged displacement of the 3′ ssDNA overhang, which could become coated in Rad51 and eventually perform strand invasion in a replication-independent manner (Figure 5, step 4). Differentiating between these and yet other possibilities remains a future goal.

It has been demonstrated that TERRA can exist in chromatin-associated fractions, as well as nucleoplasmic and cytoplasmic fractions (Porro et al., 2010), the latter two that we collectively refer to as "free" TERRA (i.e., not chromatin-associated). Rat1 is likely regulating the pool of free TERRA, because telomeric

R-loop removal is not perturbed in the absence of Rat1. Although we have carried out our analysis in telomerase-negative cells to investigate the effects of TERRA on replicative senescence, there is strong evidence that free TERRA can interact with and regulate telomerase (Cusanelli et al., 2013; Moravec et al., 2016; Redon et al., 2010). Based on these studies, we speculate that at critically short telomeres, the accumulation of free TERRA due to loss of local Rat1 function may help to recruit telomerase back to that telomere (in a *cis* manner) for subsequent elongation. The regulation of telomerase at short telomeres by Rat1 remains to be clarified.

In summary, the regulation of TERRA as a function of telomere length plays an important role in terms of telomere re-elongation. In the presence of telomerase, TERRA produced from a short telomere can associate with telomerase and assist in guiding telomerase back to the short telomere where TERRA was transcribed in order to promote elongation (Cusanelli et al., 2013; Moravec et al., 2016). In telomerase-negative cells, defective R-loop removal, specifically at critically short telomeres, activates the DDR and fosters telomere maintenance via HDR (Balk et al., 2013) (Figure 5) to buffer against early-onset replicative senescence.

STAR★METHODS

Detailed methods are provided in the online version of this paper and include the following:

- KEY RESOURCES TABLE
- CONTACT FOR REAGENT AND RESOURCE SHARING
- EXPERIMENTAL MODEL AND SUBJECT DETAILS
- METHOD DETAILS
  - Construction of the inducible very short telomere and control strains
  - Co-immunoprecipitation
  - Chromatin Immunoprecipitation and DNA-RNA Immunoprecipitation
  - SDS-PAGE and western blot
  - Yeast spotting assay onto solid agar
  - TERRA level analysis by quantitative reverse transcription and PCR
  - DNA content flow cytometry
  - Induced Very Short Telomere (VST) senescence assay
  - Southern blot
  - Telomere PCR
  - Microscopic analysis of TERRA-MS2 GFP foci
  - Senescence curve
- QUANTIFICATION AND STATISTICAL ANALYSIS

SUPPLEMENTAL INFORMATION

Supplemental Information includes four figures and three tables and can be found with this article online at http://dx.doi.org/10.1016/j.cell.2017.06.006.

AUTHOR CONTRIBUTIONS

M.G., D.B., A.L., A.M., K.S., V.K., and P.J. designed and performed experiments and analyzed data. M.T.T. and B.L. designed experiments, analyzed data, and wrote the manuscript together with M.G., D.B., and A.L.

REFERENCES

Abdallah, P., Luciano, P., Runge, K.W., Lisby, M., Géli, V., Gilson, E., and Teixeira, M.T. (2009). A two-step model for senescence triggered by a single critically short telomere. Nat. Cell Biol. *11*, 988–993.

Aguilera, A., and García-Muse, T. (2012). R loops: from transcription byproducts to threats to genome stability. Mol. Cell *46*, 115–124.

Aguilera, A., and Gómez-González, B. (2008). Genome instability: a mechanistic view of its causes and consequences. Nat. Rev. Genet. *9*, 204–217.

Arnoult, N., and Karlseder, J. (2015). Complex interactions between the DNA-damage response and mammalian telomeres. Nat. Struct. Mol. Biol. *22*, 859–866.

Arora, R., and Azzalin, C.M. (2015). Telomere elongation chooses TERRA ALTernatives. RNA Biol. *12*, 938–941.

Arora, R., Lee, Y., Wischnewski, H., Brun, C.M., Schwarz, T., and Azzalin, C.M. (2014). RNaseH1 regulates TERRA-telomeric DNA hybrids and telomere maintenance in ALT tumour cells. Nat. Commun. *5*, 5220.

Azzalin, C.M., Reichenbach, P., Khoriauli, L., Giulotto, E., and Lingner, J. (2007). Telomeric repeat containing RNA and RNA surveillance factors at mammalian chromosome ends. Science *318*, 798–801.

Balk, B., Maicher, A., Dees, M., Klermund, J., Luke-Glaser, S., Bender, K., and Luke, B. (2013). Telomeric RNA-DNA hybrids affect telomere-length dynamics and senescence. Nat. Struct. Mol. Biol. *20*, 1199–1205.

Balk, B., Dees, M., Bender, K., and Luke, B. (2014). The differential processing of telomeres in response to increased telomeric transcription and RNA-DNA hybrid accumulation. RNA Biol. *11*, 95–100.

Bianchi, A., and Shore, D. (2007). Early replication of short telomeres in budding yeast. Cell *128*, 1051–1062.

Bonetti, D., Clerici, M., Anbalagan, S., Martina, M., Lucchini, G., and Longhese, M.P. (2010). Shelterin-like proteins and Yku inhibit nucleolytic processing of Saccharomyces cerevisiae telomeres. PLoS Genet. *6*, e1000966.

Boulé, J.B., and Zakian, V.A. (2007). The yeast Pif1p DNA helicase preferentially unwinds RNA DNA substrates. Nucleic Acids Res. *35*, 5809–5818.

Bourgeron, T., Xu, Z., Doumic, M., and Teixeira, M.T. (2015). The asymmetry of telomere replication contributes to replicative senescence heterogeneity. Sci. Rep. *5*, 15326.

Campisi, J., and d'Adda di Fagagna, F. (2007). Cellular senescence: when bad things happen to good cells. Nat. Rev. Mol. Cell Biol. *8*, 729–740.

Cerritelli, S.M., and Crouch, R.J. (2009). Ribonuclease H: the enzymes in eukaryotes. FEBS J. *276*, 1494–1505.

Chawla, R., Redon, S., Raftopoulou, C., Wischnewski, H., Gagos, S., and Azzalin, C.M. (2011). Human UPF1 interacts with TPP1 and telomerase and sustains telomere leading-strand replication. EMBO J. *30*, 4047–4058.

Chon, H., Sparks, J.L., Rychlik, M., Nowotny, M., Burgers, P.M., Crouch, R.J., and Cerritelli, S.M. (2013). RNase H2 roles in genome integrity revealed by unlinking its activities. Nucleic Acids Res. *41*, 3130–3143.

Clarke, D.J., Segal, M., Jensen, S., and Reed, S.I. (2001). Mec1p regulates Pds1p levels in S phase: complex coordination of DNA replication and mitosis. Nat. Cell Biol. *3*, 619–627.

Cornelio, D.A., Sedam, H.N., Ferrarezi, J.A., Sampaio, N.M., and Argueso, J.L. (2017). Both R-loop removal and ribonucleotide excision repair activities of RNase H2 contribute substantially to chromosome stability. DNA Repair (Amst.) *52*, 110–114.

Cusanelli, E., Romero, C.A., and Chartrand, P. (2013). Telomeric noncoding RNA TERRA is induced by telomere shortening to nucleate telomerase molecules at short telomeres. Mol. Cell *51*, 780–791.

de Lange, T. (2009). How telomeres solve the end-protection problem. Science *326*, 948–952.

Epshtein, A., Potenski, C.J., and Klein, H.L. (2016). Increased spontaneous recombination in RNase H2-deficient cells arises from multiple contiguous rNMPs and not from single rNMP residues incorporated by DNA polymerase epsilon. Microb. Cell *3*, 248–254.

Fallet, E., Jolivet, P., Soudet, J., Lisby, M., Gilson, E., and Teixeira, M.T. (2014). Length-dependent processing of telomeres in the absence of telomerase. Nucleic Acids Res. *42*, 3648–3665.

Feuerhahn, S., Iglesias, N., Panza, A., Porro, A., and Lingner, J. (2010). TERRA biogenesis, turnover and implications for function. FEBS Lett. *584*, 3812–3818.

Flynn, R.L., Cox, K.E., Jeitany, M., Wakimoto, H., Bryll, A.R., Ganem, N.J., Bersani, F., Pineda, J.R., Suvà, M.L., Benes, C.H., et al. (2015). Alternative lengthening of telomeres renders cancer cells hypersensitive to ATR inhibitors. Science *347*, 273–277.

Förstemann, K., Höss, M., and Lingner, J. (2000). Telomerase-dependent repeat divergence at the 3′ ends of yeast telomeres. Nucleic Acids Res. *28*, 2690–2694.

Funk, M., Niedenthal, R., Mumberg, D., Brinkmann, K., Rönicke, V., and Henkel, T. (2002). Vector systems for heterologous expression of proteins in Saccharomyces cerevisiae. Methods Enzymol. *350*, 248–257.

Greider, C.W., and Blackburn, E.H. (1987). The telomere terminal transferase of Tetrahymena is a ribonucleoprotein enzyme with two kinds of primer specificity. Cell *51*, 887–898.

Hamperl, S., and Cimprich, K.A. (2016). Conflict resolution in the genome: how transcription and replication make it work. Cell *167*, 1455–1467.

Hardy, C.F., Sussel, L., and Shore, D. (1992). A RAP1-interacting protein involved in transcriptional silencing and telomere length regulation. Genes Dev. *6*, 801–814.

Houlard, M., Artus, J., Léguillier, T., Vandormael-Pournin, S., and Cohen-Tannoudji, M. (2011). DNA-RNA hybrids contribute to the replication dependent genomic instability induced by Omcg1 deficiency. Cell Cycle *10*, 108–117.

Huang, S.N., Williams, J.S., Arana, M.E., Kunkel, T.A., and Pommier, Y. (2017). Topoisomerase I-mediated cleavage at unrepaired ribonucleotides generates DNA double-strand breaks. EMBO J. *36*, 361–373.

Huertas, P., and Aguilera, A. (2003). Cotranscriptionally formed DNA:RNA hybrids mediate transcription elongation impairment and transcription-associated recombination. Mol. Cell *12*, 711–721.

Hug, N., and Lingner, J. (2006). Telomere length homeostasis. Chromosoma *115*, 413–425.

Hughes, T.R., Morris, D.K., Salinger, A., Walcott, N., Nugent, C.I., and Lundblad, V. (1997). The role of the EST genes in yeast telomere replication. Ciba Found. Symp. *211*, 41–47, Discussion 47–52, 71–75.

Iglesias, N., Redon, S., Pfeiffer, V., Dees, M., Lingner, J., and Luke, B. (2011). Subtelomeric repetitive elements determine TERRA regulation by Rap1/Rif and Rap1/Sir complexes in yeast. EMBO Rep. *12*, 587–593.

Jeong, H.S., Backlund, P.S., Chen, H.C., Karavanov, A.A., and Crouch, R.J. (2004). RNase H2 of Saccharomyces cerevisiae is a complex of three proteins. Nucleic Acids Res. *32*, 407–414.

Kaul, Z., Cesare, A.J., Huschtscha, L.I., Neumann, A.A., and Reddel, R.R. (2011). Five dysfunctional telomeres predict onset of senescence in human cells. EMBO Rep. *13*, 52–59.

Kim, H.D., Choe, J., and Seo, Y.S. (1999). The sen1(+) gene of Schizosaccharomyces pombe, a homologue of budding yeast SEN1, encodes an RNA and DNA helicase. Biochemistry *38*, 14697–14710.

Lazzaro, F., Novarina, D., Amara, F., Watt, D.L., Stone, J.E., Costanzo, V., Burgers, P.M., Kunkel, T.A., Plevani, P., and Muzi-Falconi, M. (2012). RNase H and postreplication repair protect cells from ribonucleotides incorporated in DNA. Mol. Cell *45*, 99–110.

Lingner, J., Cooper, J.P., and Cech, T.R. (1995). Telomerase and DNA end replication: no longer a lagging strand problem? Science *269*, 1533–1534.

Luke, B., Panza, A., Redon, S., Iglesias, N., Li, Z., and Lingner, J. (2008). The Rat1p 5′ to 3′ exonuclease degrades telomeric repeat-containing RNA and promotes telomere elongation in Saccharomyces cerevisiae. Mol. Cell *32*, 465–477.

Lundblad, V., and Szostak, J.W. (1989). A mutant with a defect in telomere elongation leads to senescence in yeast. Cell *57*, 633–643.

Marcand, S., Brevet, V., and Gilson, E. (1999). Progressive cis-inhibition of telomerase upon telomere elongation. EMBO J. *18*, 3509–3519.

McGee, J.S., Phillips, J.A., Chan, A., Sabourin, M., Paeschke, K., and Zakian, V.A. (2010). Reduced Rif2 and lack of Mec1 target short telomeres for elongation rather than double-strand break repair. Nat. Struct. Mol. Biol. *17*, 1438–1445.

Moravec, M., Wischnewski, H., Bah, A., Hu, Y., Liu, N., Lafranchi, L., King, M.C., and Azzalin, C.M. (2016). TERRA promotes telomerase-mediated telomere elongation in Schizosaccharomyces pombe. EMBO Rep. *17*, 999–1012.

Morawska, M., and Ulrich, H.D. (2013). An expanded tool kit for the auxin-inducible degron system in budding yeast. Yeast *30*, 341–351.

Moretti, P., Freeman, K., Coodly, L., and Shore, D. (1994). Evidence that a complex of SIR proteins interacts with the silencer and telomere-binding protein RAP1. Genes Dev. *8*, 2257–2269.

Nanavaty, V., Sandhu, R., Jehi, S.E., Pandya, U.M., and Li, B. (2017). Trypanosoma brucei RAP1 maintains telomere and subtelomere integrity by suppressing TERRA and telomeric RNA:DNA hybrids. Nucleic Acids Res. *45*, 5785–5796.

Ohle, C., Tesorero, R., Schermann, G., Dobrev, N., Sinning, I., and Fischer, T. (2016). Transient RNA-DNA hybrids are required for efficient double-strand break repair. Cell *167*, 1001–1013.

Pfeiffer, V., and Lingner, J. (2012). TERRA promotes telomere shortening through exonuclease 1-mediated resection of chromosome ends. PLoS Genet. *8*, e1002747.

Pfeiffer, V., Crittin, J., Grolimund, L., and Lingner, J. (2013). The THO complex component Thp2 counteracts telomeric R-loops and telomere shortening. EMBO J. *32*, 2861–2871.

Phillips, D.D., Garboczi, D.N., Singh, K., Hu, Z., Leppla, S.H., and Leysath, C.E. (2013). The sub-nanomolar binding of DNA-RNA hybrids by the single-chain Fv fragment of antibody S9.6. J. Mol. Recognit. *26*, 376–381.

Porro, A., Feuerhahn, S., Reichenbach, P., and Lingner, J. (2010). Molecular dissection of telomeric repeat-containing RNA biogenesis unveils the presence of distinct and multiple regulatory pathways. Mol. Cell. Biol. *30*, 4808–4817.

Redon, S., Reichenbach, P., and Lingner, J. (2010). The non-coding RNA TERRA is a natural ligand and direct inhibitor of human telomerase. Nucleic Acids Res. *38*, 5797–5806.

Rippe, K., and Luke, B. (2015). TERRA and the state of the telomere. Nat. Struct. Mol. Biol. *22*, 853–858.

Rondón, A.G., Jimeno, S., and Aguilera, A. (2010). The interface between transcription and mRNP export: from THO to THSC/TREX-2. Biochim. Biophys. Acta *1799*, 533–538.

Sagie, S., Toubiana, S., Hartono, S.R., Katzir, H., Tzur-Gilat, A., Havazelet, S., Francastel, C., Velasco, G., Chédin, F., and Selig, S. (2017). Telomeres in ICF syndrome cells are vulnerable to DNA damage due to elevated DNA:RNA hybrids. Nat. Commun. *8*, 14015.

Sollier, J., and Cimprich, K.A. (2015). Breaking bad: R-loops and genome integrity. Trends Cell Biol. *25*, 514–522.

Soudet, J., Jolivet, P., and Teixeira, M.T. (2014). Elucidation of the DNA end-replication problem in Saccharomyces cerevisiae. Mol. Cell *53*, 954–964.

Teixeira, M.T. (2013). Saccharomyces cerevisiae as a model to study replicative senescence triggered by telomere shortening. Front. Oncol. *3*, 101.

Teixeira, M.T., Arneric, M., Sperisen, P., and Lingner, J. (2004). Telomere length homeostasis is achieved via a switch between telomerase- extendible and -nonextendible states. Cell *117*, 323–335.

Wotton, D., and Shore, D. (1997). A novel Rap1p-interacting factor, Rif2p, cooperates with Rif1p to regulate telomere length in Saccharomyces cerevisiae. Genes Dev. *11*, 748–760.

Xu, Z., Duc, K.D., Holcman, D., and Teixeira, M.T. (2013). The length of the shortest telomere as the major determinant of the onset of replicative senescence. Genetics *194*, 847–857.

Yu, T.Y., Kao, Y.W., and Lin, J.J. (2014). Telomeric transcripts stimulate telomere recombination to suppress senescence in cells lacking telomerase. Proc. Natl. Acad. Sci. USA *111*, 3377–3382.

STAR★METHODS

KEY RESOURCES TABLE

REAGENT or RESOURCE	SOURCE	IDENTIFIER
Antibodies		
Mouse monoclonal S9.6 anti-RNA-DNA hybrid	Kerafast	Cat#ENH001
Rabbit polyclonal anti-Rad51	Thermo Fisher	Cat#PA5-34905: RRID: AB_2552256
Rabbit polyclonal anti-Sic1 (FL-284)	Santa Cruz	Cat#sc-50441; RRID: AB_785671
Mouse monoclonal anti-Phosphoglycerate Kinase (22C5D8)	Invitrogen	Cat#459250; RRID: AB_2532235
Mouse monoclonal anti-Rad53	gift from M. Foiani	N/A
Mouse monoclonal anti-FLAG M2	Sigma-Aldrich	Cat#F3165; RRID:AB_259529
Rabbit polyclonal anti-Clb2 (y-180)	Santa Cruz	Cat#sc-9071; RRID: AB_667962
Rabbit polyclonal anti-Sir2 (y-80)	Santa Cruz	Cat#sc-25753; RRID: AB_656457
Mouse monoclonal anti-RNA polymerase II CTD repeat YSPTSPS (8WG16) - ChIP grade	abcam	Cat#ab817; RRID: AB_306327
Rabbit polyclonal anti-RNA polymerase II CTD repeat YSPTSPS (phospho S2) – ChIP grade	abcam	Cat#ab5095; RRID: AB_304749
Rabbit Peroxidase Anti-Peroxidase soluble complex	Sigma-Aldrich	Cat#P1291; RRID: AB_1079562
Mouse monoclonal anti-MYC-tag (9B11)	Cell Signaling/NEB	Cat#2276S; RRID: AB_331783
Mouse monoclonal anti-HA.11 (16B12)	Covance	MMS-101P-1000; RRID: AB_291259
Rabbit polyclonal anti-Rnr3	Agrisera Antibodies	Cat#AS09 574; RRID: AB_1966947
Goat Immun-Star anti-mouse (GAM)-HRP conjugate	Bio-Rad	Cat#170-5047; RRID: AB_11125753
Goat Immun-Star anti-rabbit (GAR)-HRP conjugate	Bio-Rad	Cat#170-5046; RRID:AB_11125757
Chemicals, Peptides, and Recombinant Proteins		
Formaldehyde 37%	AppliChem	Cat#A0877,0500
Glycine	AppliChem	Cat#A1067,1000
alpha-factor	Zymo Research	Cat#Y1001
Hydroxyurea	Sigma-Aldrich	Cat#H8627-25G
Nocodazole	Sigma-Aldrich	Cat#M1404-10MG
Methyl methanesulfonate	Sigma-Aldrich	Cat#129925-25G
Phenol	Sigma-Aldrich	Cat#77608-500G
Phenol stabilized: Chloroform: Isoamyl Alcohol 25:24:1	AppliChem	Cat#A2279,0500
Concanavalin A	Sigma-Aldrich	Cat#L7647-25MG
2-mercaptoethanol	Sigma-Aldrich	Cat#M6250-250ML
cOmplete EDTA-free Protease Inhibitor Cocktail	Roche	Cat#4693159001
SYTOX Green	Thermo Scientific	Cat#S7020
nProtein A Sepharose 4 Fast Flow	GE Healthcare	Cat#17-5280-01
IgG Sepharose 6 Fast Flow	GE Healthcare	Cat#17-0969-01
Protein G Sepharose 4 Fast Flow	GE Healthcare	Cat#17-0618-01
Pierce Anti-HA Magnetic Beads	Thermo Scientific	Cat#88836
SuperScript III Reverse Transcriptase	Invitrogen	Cat#18080044
dATP, [α-^{32}P]	Perkin Elmer	Cat#NEG512H100UC
Restriction enzyme XhoI	NEB	Cat#R0146L
Restriction enzyme EcoRI-HF	NEB	Cat#R3101S
DNase I	QIAGEN	Cat#79254
RNase A	Thermo Scientific	Cat#EN0531
Proteinase K	QIAGEN	Cat#19133

(Continued on next page)

Continued

REAGENT or RESOURCE	SOURCE	IDENTIFIER
SuperSignal West Pico Chemiluminescent Substrate	Thermo Scientific	Cat#34087
SuperSignal West Dura Chemiluminescent Substrate	Thermo Scientific	Cat#34076
Critical Commercial Assays		
QIAquick PCR Purification Kit	QIAGEN	Cat#28106
RNeasy MinElute Cleanup Kit	QIAGEN	Cat#74204
DyNAmo Flash SYBR Green qPCR Kit	Thermo Scientific	Cat#F415XL
DECAprime II DNA Labeling Kit	Thermo Scientific	Cat#AM1455
Experimental Models: Organisms/Strains		
S. cerevisiae standard laboratory strain S288C derivatives, see Table S1	This study	N/A
S. cerevisiae standard laboratory strain W303 derivatives, see Table S1	This study	N/A
S. cerevisiae standard laboratory strain FY23 derivatives, see Table S1	This study	N/A
Oligonucleotides		
Primers for PCR and qPCR, see Table S2	This study	N/A
Recombinant DNA		
Plasmid: pRS423 pGAL, 2μ	(Funk et al., 2002)	pBL186
Plasmid: pRS423 pGAL-HA-RNH201, 2μ	This paper	pBL188
Plasmid: pRS426 pGPD, 2μ	(Balk et al., 2013)	pBL189
Plasmid: pRS426 pGPD-RNH1-HA, 2μ	(Balk et al., 2013)	pBB39
Plasmid: pRS425 pGAL-RNH1-HA, 2μ	This Study	pBL352
Plasmid: pRS425 pGAL, 2μ	(Funk et al., 2002)	pBL211
Plasmid: pGPD-MS2BP-GFP, 2μ	(Cusanelli et al., 2013)	pBL449
Plasmid: pGPD, CEN	(Funk et al., 2002)	pBL335
Plasmid: pGPD-RNH1-HA, CEN	This paper	pBL336
Plasmid: pSP100, contains probe for Southern Blot	Kind gift from M.P. Longhese	pBL423
Plasmid: 6R ctrl construct	This study	pT26
Plasmid: 6R VST construct	This study	pT29
Plasmid: pRS316, CEN	(Funk et al., 2002)	pBL97
Plasmid: pRS316 rnh201-P45D-Y219A, CEN	This study	pBL399
Software and Algorithms		
Prism 7	GraphPad software	https://www.graphpad.com/scientific-software/prism/
FACSuite 1.0.5	Becton Dickinson	http://www.bdbiosciences.com/eu/instruments/research/software/flow-cytometry-acquisition/bd-facsuite-software/m/111113/overview
Image Lab 5.2	Bio-Rad	http://www.bio-rad.com/en-us/product/image-lab-software
ImageJ 1.50a	NIH	https://imagej.nih.gov/ij/download.html
Bio-Rad CFX Manager 3.1	Bio-Rad	http://www.bio-rad.com/de-de/sku/1845000-cfx-manager-software

CONTACT FOR REAGENT AND RESOURCE SHARING

Further information and requests for resources and reagents should be directed to and will be fulfilled by the Lead Contact, Brian Luke (b.luke@imb-mainz.de).

EXPERIMENTAL MODEL AND SUBJECT DETAILS

Saccharomyces cerevisiae strains used in this paper are derivatives of the standard strains S288C, W303 or FY23 and are listed in Table S1.

Strains were grown under standard conditions in YPD (Yeast Peptone Dextrose) or SC without amino acids (Synthetic Complete) at 30°C if not indicated otherwise. Further specifications are mentioned within the Methods Details section.

METHOD DETAILS

Construction of the inducible very short telomere and control strains

To construct yT361 and yT362 containing the single telomere shortening system at chromosome 6R, the SphI-HindIII *adh4* region contained in sp225 and sp242 (Marcand et al., 1999) was replaced by a PCR fragment containing a 0,5 kb region of the 6R chromosome end next to telomeric repeats to obtain pT26 and pT29, respectively. This fragment was obtained by PCR on genomic DNA using the oligonucleotides oT346 and oT347. yT360 was obtained by transforming W303-1A by sp200 (Marcand et al., 1999). The 6R-CTL and VST strains were obtained by transforming yT360 by plasmids pT26 (6R-CTL; yT361) and pT29 (6R-VST; yT362) digested with SphI and NotI. Transformants were verified by pulse field gel electrophoresis and Southern blot. For each chromosome plug, 5.10^7 exponentially growing cells were washed in 10 mM Tris 50 mM EDTA pH 8 and molded in Biorad plug molds in prewarmed (42°C) 1% low melting agarose (QA-Agarose Cat# AGAL0050 MPbio/qbiogene) in Zymolyase buffer (50 mM potassium phosphate 50 mM EDTA, pH 8). After solidification (30 min at 4°C), plugs are incubated in zymolyase buffer containing 10 mM DTT 0.4 mg/ml, Zymolyase 20T (Seikagaku) overnight at 37°C. This buffer is then replaced by Proteinase K buffer (10 mM Tris pH 7.5, 50 mM EDTA, 1% Sarkosyl, 2 mg/ml proteinase K (Sigma P2308)) and incubated further 24h at 50°C. Plugs are extensively washed in 10 mM Tris, 50 mM EDTA, pH 8. Plugs were run in 0.9% agarose 0.3x TBE gel in a Rotaphor apparatus (Biometra) with the 3-1600 kb 24h program (T°C: 13°C; interval: 100 > 10 (Log); angle: 120 > 110 (Lin); voltage: 200 > 150 (Log)). Gels were then stained with 0.5 microg/ml Ethidium bromide, photographed and processed as a Southern Blot. For the Southern blot genomic DNA was restriction digested and electrophoresed in a 1% agarose gel 0.5x TBE 16-20h at 60 V. The gel was then incubated 15 min in 0.25 M HCl, 20 min in 0.4 M NaOH, 1 M NaCl and then transferred onto nylon membrane (XL Hybond) with 0.4 M NaOH, 1 M NaCl by capillarity. The membrane was soaked 15 min in 0.5 M Tris pH7.5, 1 M NaCl, air-dried and UV crosslinked 120 mJ/ cm2. Hybridization was done at 65°C in Church buffer (0.5 M Sodium Phosphate, 0.5 M EDTA, 20% SDS, 1% BSA) containing a denatured probe labeled by random priming of a SphI-NotI fragm,ent of sp26 (Klenow 3′-5′exo- cat#M0212 from NEB) with [α-32P]dATP. The membrane was washed 3 times 15 min with Church washing buffer (0.5 M Sodium Phosphate, 20% SDS) and exposed to a phosphorimager screen and revealed in Typhoon FLA 9500 (GE Healthcare).

yT361 and yT362 were then crossed with yT367 and sporulated. Ura+ Trp+ Nat^R spores were dubbed yT483 and yT484 and backcrossed with yT361 and yT362 to obtain yT502 and yT503, respectively.

Co-immunoprecipitation

Yeast cells were grown to OD_{600} 0.8-1, either untreated or arrested with alpha-factor or HU in 100 mL selective media and subsequently centrifuged. Cell pellets were resuspended in IP buffer (50 mM Tris pH 7.5, 150 mM (Figure S4D) or 300 mM (Figure 4A) NaCl, 5 mM MgCl$_2$, 1 mM PMSF, protease inhibitor cocktail) and cells were lysed with lysing Matrix C tubes via FastPrep (MP Biomedicals; 6.5 M/s, 2 × 30 s with 1 min on ice between runs). Cell extracts were recovered by addition of IP buffer + 0.2% NP40, and centrifuged twice recovering the supernatant. Cell extracts were diluted to 2 mg/ml of proteins in IP buffer + NP40. 2.5% of the IP volume was diluted in urea buffer and used as input. IP samples were incubated with prewashed Pierce anti-HA Magnetic beads (Thermo Scientific; washed twice with IP buffer + NP40) and 4 μl DNase I (QIAGEN) for 2 hr at room temperature. IPs were then washed 4 times for 5 min each with IP buffer + NP40 at 4°C, and then resuspended in urea buffer. IP and input samples were subsequently boiled at 95°C for 7 min 30 s and loaded on a gel for western blotting with the indicated antibodies.

Chromatin Immunoprecipitation and DNA-RNA Immunoprecipitation

Yeast cells in exponential growth phase or arrested in specific cell cycle stages with either alpha-factor, HU or nocodazole (OD_{600} 0.6-1) were diluted to the same OD_{600} values, crosslinked for 10 min (15 min for Rnh201-TAP) with formaldehyde (final conc. 1.2%) and quenched with glycine (360 mM final) for 5 min. After incubation on ice for at least 5 min, cells were pelleted and washed twice with 1 × PBS, resuspended in FA lysis buffer (50 mM HEPES-KOH pH 7.5, 140 mM NaCl, 1 mM EDTA pH 8, 1% Triton X-100, protease inhibitor cocktail) and lysed with lysing Matrix C tubes via FastPrep (MP Biomedicals; 6.5 M/s, 2x 30 s with 1 min on ice between runs). Cell extracts were recovered adding FA lysis buffer containing 0.1% sodium deoxycholate (SOD), centrifuged and the soluble portion of the lysate was discarded. Pellets were resuspended in FA lysis buffer with SOD + SDS (0.263% final). Chromatin was sheared 30 s on/off for 19 cycles at 4°C with Bioruptor Pico (Diagenode). After centrifugation, the supernatant (ChIP extract) was diluted to 1 mg/ml protein concentration in FA lysis buffer + SOD and used for immunoprecipitation (IP). An input sample representing 5% of the ChIP extract used for IP served for normalizing the qPCR. To verify sonication efficiency, a sample of ChIP extract was

incubated overnight at 65°C and treated with proteinase K (QIAGEN; 0.75 mg/ml) for 2 hr at 37°C. The sample was purified with QIAquick PCR Purification Kit (QIAGEN), treated with RNase A solution (Thermo Scientific) for 30 min at 37°C and analyzed on a 1.5% agarose gel.

All beads used for IPs were washed with 1 × PBS, FA lysis buffer and pre-incubated with 5% BSA for 1 hr at 4°C.

For DRIP, 1 mg/ml extracts were precleared with nProtein A Sepharose 4 Fast Flow beads (GE Healthcare) for 1 hr at 4°C. IP was performed overnight at 4°C with nProtein A beads in the presence or absence of 2-3 μg of S9.6 antibody (Kerafast).

For MYC ChIP, nProtein A Sepharose 4 Fast Flow beads (GE Healthcare) were used; after preclearing, 3 μl anti-myc antibody (Cell Signaling/NEB) were added to each sample with fresh protein A beads and incubated overnight at 4°C.

For TAP ChIPs (Rat1, Rnh1 and Rnh201) IgG Sepharose 6 Fast Flow beads (GE Healthcare) were used and the IP was performed overnight at 4°C.

For RNAPII ChIPs (total RNAPII and phospho-serine2 RNAPII; abcam; 5 μg each per IP), nPprotein A Sepharose 4 Fast Flow beads (GE Healthcare) were used.

For the Rad51 ChIP (Thermo Fisher; 2 μl antibody per 1 mg ChIP extract) Protein G Sepharose 4 Fast Flow beads (GE Healthcare) were used. For the Sir2 ChIP (Santa Cruz; 10 μl per 1 mg ChIP extract) Protein G Sepharose 4 Fast Flow beads were used.

Beads were washed with: FA lysis buffer + SOD, FA lysis buffer 500 (FA lysis buffer with 500 mM NaCl), buffer III (10 mM Tris-HCl, pH 8.0, 1 mM EDTA, pH 8.0, 250 mM LiCl, 1% Nonidet P-40 and 1% sodium deoxycholate) and TE (pH 8.0). All washing steps were performed for 5 min at 4°C. Bead-bound DNA was eluted twice in 100 μl elution buffer B (50 mM Tris-HCl, pH 7.5, 1% SDS, 10 mM EDTA, pH 8.0) for 8 min at 65°C. For reverse-crosslinking, IPs and input were treated overnight at 65°C with proteinase K (QIAGEN; 0.75 mg/ml). DNA was cleaned with QIAquick PCR Purification Kit (QIAGEN).

qPCR analysis was performed using CFX384 Touch Real-Rime PCR Detection System (Bio-Rad) and SYBR-Green (Thermo Scientific) detection with 60°C annealing temperature, all oligonucleotides used are listed in Table S2. Measured Cq values were corrected to input. Graphs were created with Prism7 (GraphPad).

SDS-PAGE and western blot

Culture volumes corresponding to 2 OD_{600} units were collected by centrifugation at 13,000 rpm for 2 min. Cell pellets were resuspended with 150 μl solution 1 (1.85 M NaOH, 1.09 M 2-mercaptoethanol) and incubated on ice for 10 min. 150 μl solution 2 (50% TCA) were added before further incubation on ice for 10 min. Cells were centrifuged at 13,000 rpm for 2 min at 4°C, the pellet resuspended with 1 mL acetone, and centrifuged again at 13,000 rpm for 2 min at 4°C. The pellet was resuspended in 100 μl urea buffer (120 mM Tris-HCl pH 6.8, 5% glycerol, 8 M urea, 143 mM 2-mercaptoethanol, 8% SDS, bromophenol blue indicator) and incubated for 5 min at 75°C. Samples were loaded on pre-cast 4%–15% gels (Bio-Rad). The following antibodies were used: anti-HA (Covance) at 1:2,000; anti-MYC (Cell Signaling/NEB) at 1:1,000; anti-Pgk1 (Invitrogen) at 1:200,000; PAP (Sigma-Aldrich) 1:1,000; anti-FLAG M2 (Sigma Aldrich) at 1:1000, anti-Clb2 (Santa Cruz) at 1:1000, anti-Sic1 (Santa Cruz) at 1:500, anti-Rad53 (gift from Marco Foiani) at 1:1000 and anti-Rnr3 (Agrisera Antibodies) at 1:300. Proteins were detected using the Super Signal West Pico Chemiluminescent Substrate (Thermo Scientific) or the Super Signal West Dura Extended Duration Substrate (Thermo Scientific) on Bio-Rad ChemiDoc Touch Imaging System.

Yeast spotting assay onto solid agar

For spotting assays, yeast cells were incubated overnight at 30°C in YPD. Cells were diluted to OD_{600} 0.5 and spotted in ten-fold dilutions onto YPD plates or YPD plates containing 0.04% MMS (Sigma-Aldrich). Plates were then incubated at the indicated temperatures and time and imaged using the Bio-Rad ChemiDoc Touch Imaging System.

TERRA level analysis by quantitative reverse transcription and PCR

10 OD_{600} units of exponentially growing cells were used to extract RNA. The pellet was resuspended in 400 μl AE buffer (50 mM sodium acetate, 10 mM EDTA, pH 5.3) and incubated with 500 μl phenol (equilibrated with AE buffer) at 65°C for 5 min. After chilling on ice for 5 min, the organic and aqueous phase were separated by centrifugation for 3 min at 13,300 rpm. The aqueous phase was mixed with 500 μl phenol-chloroform-isoamyl alcohol and incubated for 5 min at room temperature. The phases were again separated. RNA was precipitated from the aqueous phase with 40 μl 3 M sodium acetate and 1 mL ice-cold 100% ethanol. The RNA was pelleted and washed once in 80% ethanol. The air-dried pellet was resuspended in 87 μl water, 10 μl RDD buffer, 3 μl DNase I (QIAGEN) and 1 μl RNaseOUT (Invitrogen). Genomic DNA was digested for 45 min at 37°C. 50 μg total RNA were digested two more times with DNase I with clean-up steps by the RNeasy MinElute Cleanup kit (QIAGEN). 3 μg DNase I digested RNA were subjected to reverse transcription. The RNA was incubated with 0.4 μl 25 mM dNTPs, 1 μl 10 μM oBL207, 0.4 μl 10 μM oBL293 in a total volume of 10 μl at 90°C for 1 min and cooled down to 55°C with a rate of 0.8°C/s. 1 μl 0.1 M DTT, 1 μl RNaseOUT, 4 μl 5x FS-buffer and 1 μl SuperScript III (Invitrogen) were added to the reaction. The reverse transcription took place at 55°C for 60 min. The reaction was stopped at 70°C for 15 min. 30 μl water were added to the sample. qPCR analysis was performed as mentioned above. TERRA levels were normalized to respective actin values and correlated to the wild-type.

DNA content flow cytometry

0.18 OD_{600} units were fixed in 70% ethanol for 1 hr at room temperature or overnight at 4°C. The fixed cells were washed once in 800 µl 50 mM sodium citrate (pH 7.4). Afterward the cells were resuspended in 500 µl sodium citrate supplemented with 0.25 mg/ml RNase A (Thermo Scientific). RNA was degraded for 2 to 3 hr at 37°C. 25 µl proteinase K (QIAGEN) were added for another 1 to 2 hr and the samples were incubated at 50°C. The cells were then sonicated three times for 5 s using the Bioruptor Pico (Diagenode). 500 µl sodium citrate supplemented with 4 µM SYTOX Green (Thermo Scientific) were added before the DNA content was measured with BD FACSVerse.

Induced Very Short Telomere (VST) senescence assay

The senescence assay was performed as described (Fallet et al., 2014). Briefly, yBB271 and yBB272 and their derivatives containing plasmids are mass sporulated and germinated in the presence of galactose rich medium for 6-9 hr. To control induction, germination of the same sporulation mixture is also performed in glucose–containing media. Telomerase-negative spores are selected by plating the germination mixture on Nourseothricin-containing media. After 2 days, a small portion of the colonies is used to genotype and to verify the loss of the URA3 marker and telomere length by telomere-PCR (see below) (Förstemann et al., 2000). Remaining cells are then re-suspended, adjusted to the same concentration, serially diluted 10-fold and then spotted on solid media, followed by a two-days-incubation at 30°C (passage 1). This procedure is repeated every two days using mixed cells from the most concentrated spot until complete loss of viability, typically 2 times (passage 2 and passage 3). Plates are scanned with an Epson Perfection V750 Pro and analyzed to obtain the viability plots: For each clone and each passage, the signal intensity of each spot was measured using the 'Microarray Profile' plugin of ImageJ 1.46a. Signal intensity versus dilution could then be plotted. A threshold value of the intensity was set to correspond to an exponentially growing strain (here, one-fifth of the maximum intensity of cells grown to saturation) and used for all experiments. The viability index is the theoretical dilution necessary to obtain a spot intensity equal to the threshold value. Negative values were obtained by extrapolation of the curve, and the minimum value was limited to 10. Viability indexes for each genotype were plotted as boxplots using R2.15.2. P values were determined using pairwise Wilcoxon rank-sum tests and adjusted with a false discovery rate correction. At least two complete independent experiments were performed and one is shown.

Southern blot

Genomic DNA was extracted from respective yeast cultures. 5 µg DNA were digested with XhoI for 5 hr at 37°C. The complete 5 µg were loaded onto a 0.8% agarose gel. Electrophoresis took place overnight at 50 V. The DNA in the gel was denatured for 1 hr (0.4 M NaOH, 0.6 M NaCl) and then neutralized again for 1 hr (1 M Trizma Base, 1.5 M NaCl, pH 7.4). The DNA was transferred to a nylon membrane (Hybond-NX, GE Healthcare) via capillary transfer in 10x SSC overnight and cross-linked to the membrane with UV light (auto X-link, Stratalinker). The membrane was pre-hybridized in hybridization solution for 5 hr at 55°C (0.5 M $NaPO_4$, 1 mM EDTA, 7% SDS, 1% BSA). The telomere-specific probe was generated by random primed radioactive labeling with dATP [α-^{32}P] (DECAprime kit II; Thermo Scientific) of a double-stranded DNA fragment obtained by digestion of pBL423 with EcoRI followed by gel extraction. Hybridization took place overnight at 55°C. The membrane was washed twice in pre-warmed washing solution (0.2 M $NaPO_4$, 1% SDS) (for 1 hr and 30 min, respectively) before the membrane was air-dried for 30 min. The film was exposed to the blot for two to three days and detected via Typhoon FLA 9500 (GE Healthcare).

Telomere PCR

1 µl 100 ng/µl genomic DNA was mixed with 7.1 µl water and 0.9 µl NEB4 buffer. The solution was boiled for 10 min at 96°C before it was cooled down to 4°C. Afterward, 0.2 µl terminal transferase (New England Biolabs), 0.1 µl NEB4 buffer, 0.1 µl 10 mM dCTP and 0.6 µl water were added. The C-tailing reaction was allowed to take place for 30 min at 37°C, before the reaction was heated up to 65°C for 10 min and afterward to 96°C for 5 min. Thereafter, the PCR mix was added (21 µl water, 4 µl 10x PCR buffer (670 mM Tris-HCl pH 8.8, 160 mM $(NH_4)SO_4$, 50% glycerol, 0.1% Tween-20, in water), 4 µl 2 mM dNTPs, 0.3 µl 100 µM oT531, 0.3 µl 100 µM oBL359, 0.4 µl Phusion HF (New England Biolabs)). The PCR program was as follows: 98°C for 3 min, 98°C for 30 s, 63°C for 15 s, 72°C for 20 s (last three steps repeated 44 times), 72°C for 5 min. The PCR products were analyzed via gel electrophoresis on a 1.8% agarose gel.

Microscopic analysis of TERRA-MS2 GFP foci

To detect TERRA foci as previously described (Cusanelli et al., 2013), cells were inoculated overnight in an appropriate medium. Cells were diluted to an OD_{600} of 0.1 and allowed to double once. 0.06 OD_{600} units were transferred to concanavalin A (Sigma-Aldrich) coated microscopy chambers. TERRA and Rap1-mCherry foci were detected using a Leica AF7000 widefield fluorescence microscope with a 63x/1.4 NA oil immersion objective. Images were taken with Hamamatsu Orca R2 (CCD) and analyzed with ImageJ 1.50a (Bio-Formats plugin).

Senescence curve

Liquid senescence assays were performed as in Balk et al., 2013. After dissection, cells were grown in 5 mL selective media or YPD at 30°C and the starting OD_{600} was set to 0.01 each day. Population doublings were calculated each day as the $log_2(OD_{600}/0.01)$, where

the OD_{600} is the cell density measured after 24 hr. Graphs were plotted using Prism7. The heterozygous diploid strain yVK1290 was transformed with either pBL97 or pBL399 prior to dissection on selective plates.

QUANTIFICATION AND STATISTICAL ANALYSIS

Statistical parameters are reported in the Figures and the Figure Legends.
  p values calculated for the VST spotting assay are listed in Table S3 (related to Figure 2H).
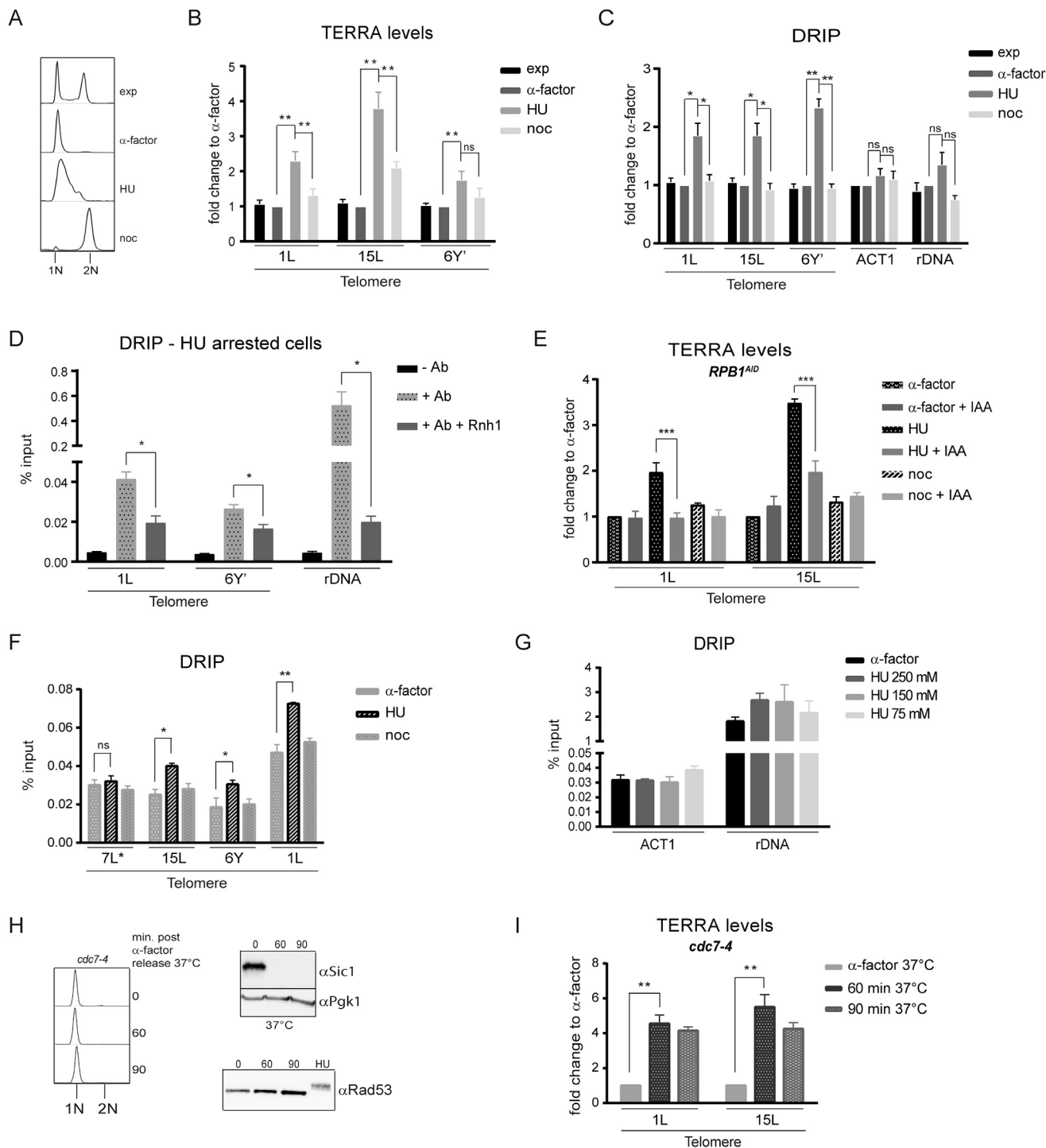
Supplemental Figures

Figure S1. TERRA and RNA-DNA Hybrid Increase during S Phase in a Transcription-Dependent Manner, Related to Figure 1

(A–C) TERRA and RNA-DNA hybrids are cell cycle regulated. Wild-type cells were grown to exponential phase (exp) and synchronized in G1 with α-factor pheromone, in S phase with 200 mM HU and at G2/M with 15 μg/ml nocodazole for 3 hr. (A) DNA content was measured by FACS. (B) Total RNA was extracted and reverse transcribed. TERRA molecules originated from specific telomeres (1L, 15L and 6Y' containing telomeres) were analyzed by qPCR. Values are represented as percentage of *ACT1* total RNA and relative to cells arrested in α-factor, which is set to 1 for each primer set. Data are depicted as mean + SEM of 3 biological replicates. (C) DRIP. Chromatin was immunoprecipitated using the RNA-DNA hybrid-specific S9.6 antibody and analyzed by qPCR at the indicated loci. Values are represented as percentage input of DNA recovered relative to cells arrested in α-factor, which is set to 1 for each primer set. Data are depicted as mean + SEM of 3 biological replicates.

(legend continued on next page)

(D) DRIP extracts from HU arrested cells were treated with 50 U of recombinant RNase H and DRIP was executed and analyzed as in (C).

(E) Increase in TERRA levels during S phase is transcription dependent. Cells carrying an auxin-inducible degron variant of the large subunit of the RNA poly-merase II ($RPB1^{AID}$) were synchronized in G1 with α-factor pheromone, in S phase with 200 mM HU and at G2/M with 15 μg/ml nocodazole for 3 hr. Indole-acetic acid (IAA) was added to half of the culture to 500 μM final concentration for 1 hr to induce Rpb1 depletion. TERRA molecules were measured as in (B).

(F) TERRA forms R-loops in S phase. A strain carrying a modified telomere 7L (7L*) was grown to exponential phase and synchronized as in (B). DRIP analysis was performed as in (C), but values are represented as percentage input of telomeric DNA recovered. Data are shown as mean + SEM of 3 biological replicates.

(G) Wild-type cells were synchronized in G1 with α-factor pheromone for 2 hr and then released into the cell cycle at 30°C in the presence of the indicated concentrations of HU. DRIP analysis was performed as in (F) with the indicated amplicons. (H and I) In S phase TERRA levels increase independently of checkpoint activation. Cells carrying a temperature sensitive allele of $CDC7$ ($cdc7-4$) were arrested in G1 with α-factor for 2 hr at 25°C and then shifted to 37°C for 1 hr. Part of the culture was then released into S phase at 37°C for the indicated time points.

(H) DNA content analysis by FACS and western blot analysis of Sic1 protein levels and Rad53 phosphorylation status. Pgk1 protein levels were measured as a loading control.

(I) TERRA levels were analyzed as in (B). For all experiments p values were obtained from two-tailed Student's t tests (*$p < 0.05$, **$p < 0.01$).
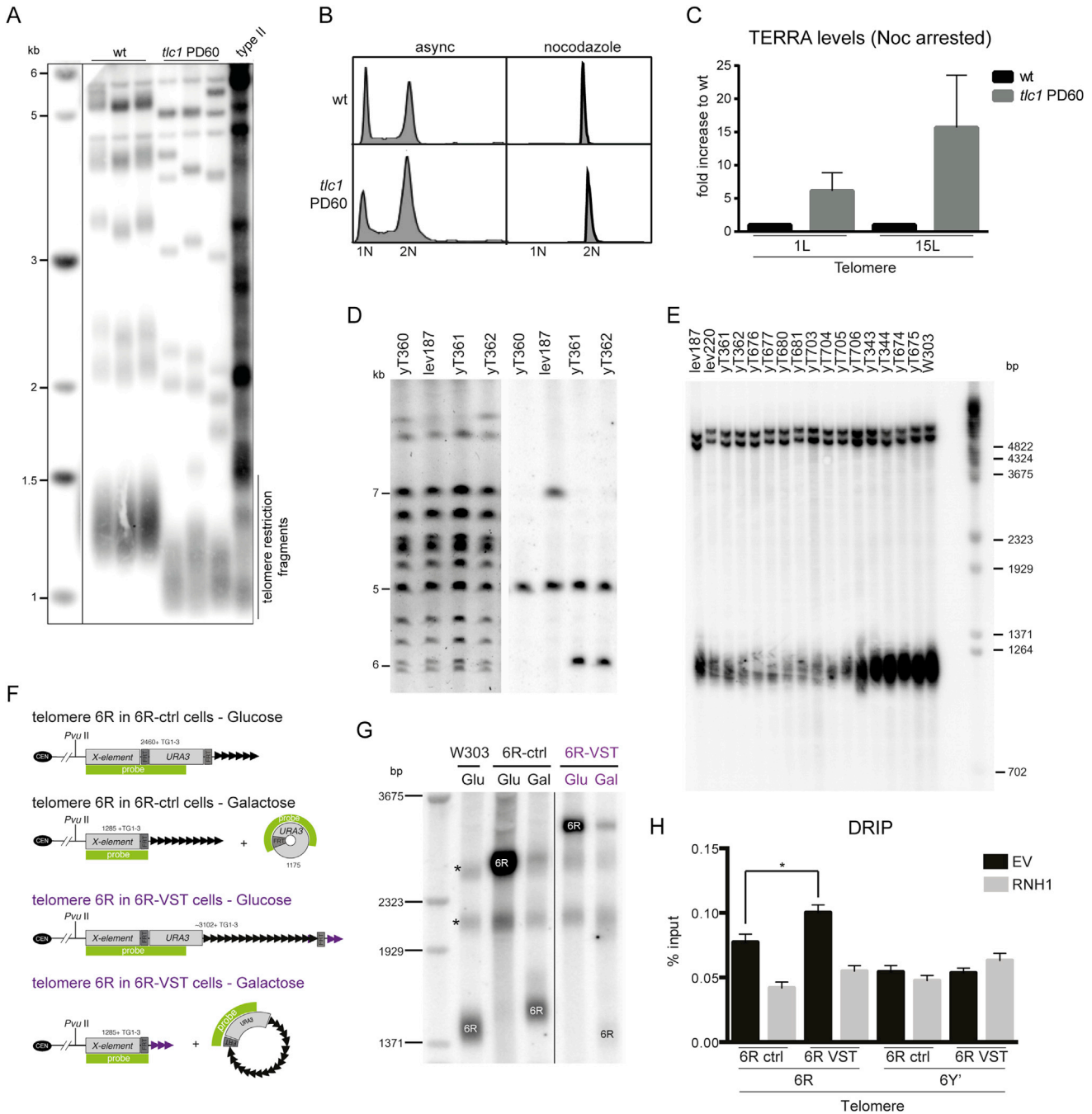
Figure S2. Critically Short Telomeres Accumulate TERRA and R-Loops, Related to Figure 2

(A) TERRA and RNA-DNA hybrid levels increase independently of survivor formation. For the Southern blot DNA of the indicated strains used in Figures 2A and 2B, DNA was extracted and digested with XhoI. The blot was hybridized with a radioactive probe recognizing telomeric DNA. As a control, one type II survivor was loaded. Vertical line next to the DNA ladder indicates cropping of superfluous lanes.

(B) Cell cycle analysis of depicted genotypes in an asynchronous culture and after G2/M arrest with nocodazole. Samples for DNA FACS were taken from exponential phase and after a 2.5 hr treatment with 15 μg/ml nocodazole. 1N: DNA content, G1 phase; 2N: DNA content, G2/M phase. One representative histogram for each condition is shown.

(C) TERRA level increase in pre-senescent cells is independent of the cell cycle. TERRA levels in arrested cells were measured as described previously. The mean values in arrested pre-senescent cells + SEM of 3 independent experiments are depicted normalized to WT. (D-G) Verification of correct strain construction.

(D) Pulse-field gel electrophoresis of indicated strains was transferred onto a nylon membrane and hybridized with a *URA3* probe. The endogenous *URA3* locus is detected on chromosome 5. Chromosome numbers are indicated on the left.

(legend continued on next page)

(E) Lengths of Y' telomeres of indicated telomerase-positive strains were measured by Southern blot of XhoI digested genomic DNA hybridized with a Y' specific probe.

(F and G) Schematic representation of Telomere Restricted Fragment (TRF) analysis (F) and corresponding Southern blots at 6R (G). Cells were cultivated for 4 hr in a rich medium containing either glucose or galactose, to induce shortening, followed by DNA extraction and DNA restrictive digestion by PvuII. *: corresponds to cross hybridization to other X elements in the genome; 6R: 6R TRF. Vertical line between lanes 4 and 5 indicates cropping of superfluous lanes.

(H) RNA-DNA hybrid abundance is upregulated at the shortest telomere of a cell. RNA-DNA hybrid DRIP was performed as mentioned in the main figures. The mean % input values are displayed + SEM n = 3, *p < 0.05 (unpaired Student's t test).
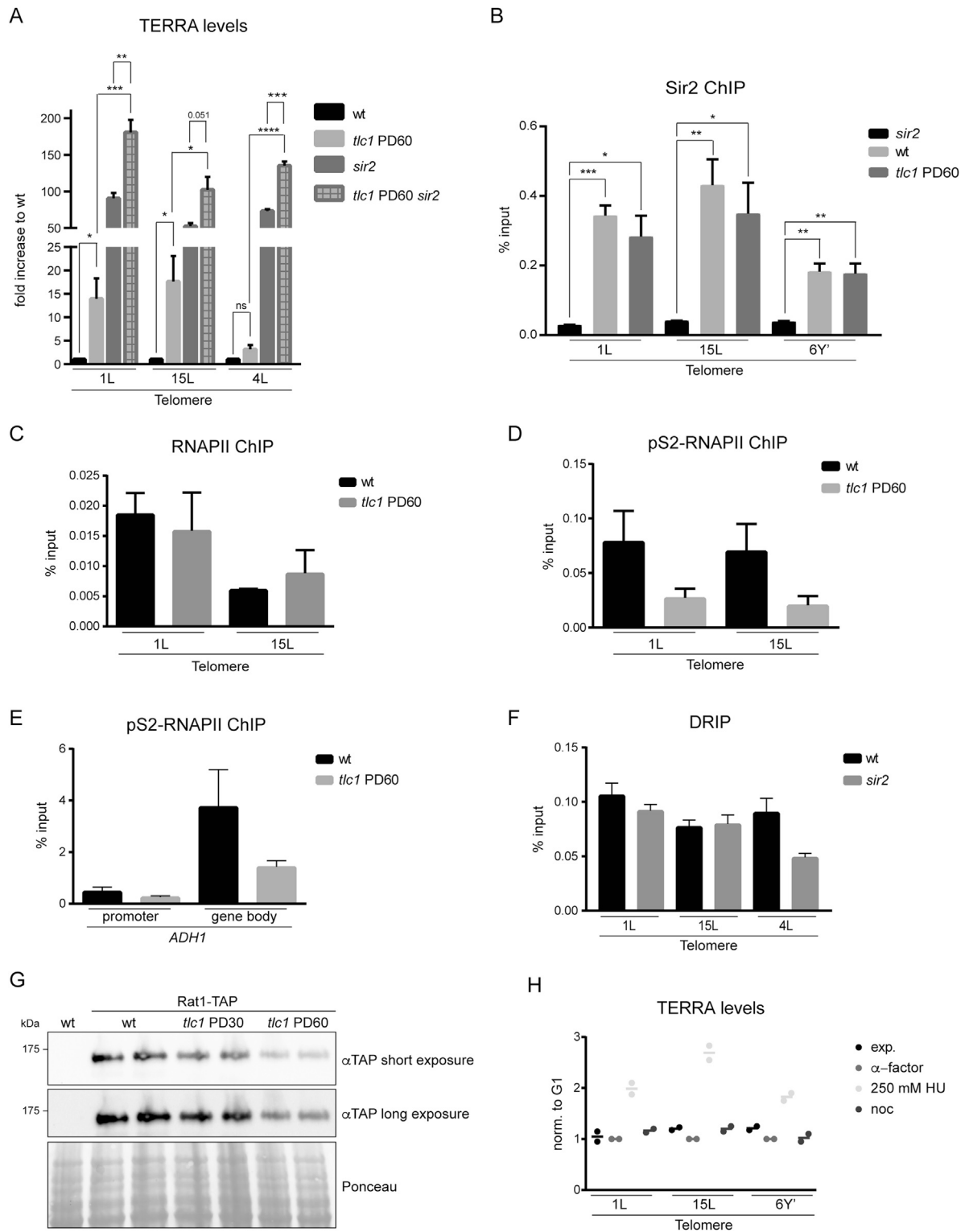
Figure S3. TERRA Level Increase Is Not Due to Loss of Silencing, Related to Figure 3

(A) TERRA level increase in *sir2* and pre-senescent *tlc1* is additive. TERRA levels were determined as described before. The mean values normalized to wild-type + SEM are displayed. n = 3, ns: not significant; *p < 0.05, **p < 0.01, ***p < 0.001).

(B) Sir2 abundance at telomeres is not strongly influenced by telomere length. A ChIP assay with crosslinked samples was performed. Sir2 was pulled down with a polyclonal antibody. The mean values are represented as + SEM n = 3; *p < 0.05, **p < 0.01, ***p < 0.001.

(C–E) ChIP assay to measure total RNA Polymerase II levels or the actively transcribing form (phosphorylated at serine 2 of the C-terminal domain). The pulldown was performed on crosslinked extracts. The mean values are displayed as + SEM n = 3.

(F) RNA-DNA hybrid levels are not influenced by Sir2 status. A DRIP on WT and *sir2* cells was performed as described before. The mean values ± SEM are represented. n = 3.

(G) Western blotting was performed to detect a TAP-tagged version of Rat1 in both non-senescent and pre-senescent cells.

(H) Total RNA was extracted and reverse transcribed. TERRA molecules originated from specific telomeres (1L, 15L and 6Y' containing telomeres) were analyzed by qPCR. Values are represented as percentage of *ACT1* total RNA and relative to cells arrested in α-factor, which is set to 1 for each primer set. 2 biological replicates.

A

B

YPD   0.04% MMS

wt
rnh1
rnh201
RNH1-TAP
RNH201-TAP
rnh1rnh201
rnh1 RNH201-TAP
RNH1-TAP *rnh201*

C

Rnh201-TAP

exp exp α-factor HU 250 mM HU 75 mM

αTAP
αSic1
αPgk1

D

INPUT   IP-HA

αmyc

αHA

E

Rnh201-TAP

kDa   wt   *rif2*   *rif1*
80
58   αTAP
58
46   αPgk1

F

Rnh1-TAP ChIP

relative % input

■ wt   ■ Rnh1-TAP

1L   15L   6Y'
Telomere

G

Rat1-TAP ChIP

relative % input

■ wt
■ Rat1-TAP
□ Rat1-TAP *rif1*
▨ Rat1-TAP *rif2*
▤ Rat1-TAP *rif1 rif2*

1L   15L   6R   6Y'   actin
Telomere

H

YPD   0.04% MMS

wt
rnh1
rnh201
rif2
rnh1 rnh201
rnh1 rif2
rnh201 rif2
rnh1 rnh201 rif2

I

RIF2^{AID}   *RIF1^{AID}*   *RIF2^{AID}* *RIF1^{AID}*

kDa   -   +   -   +   -   +   IAA

190   Rif1   αmyc

58   Rif2

46   αPgk1

J

DRIP

relative % input

■ wt   ■ *rif2*

RNH1 - + - +   - + - +   - + - +   - + - +
        1L   15L   6Y'   rDNA
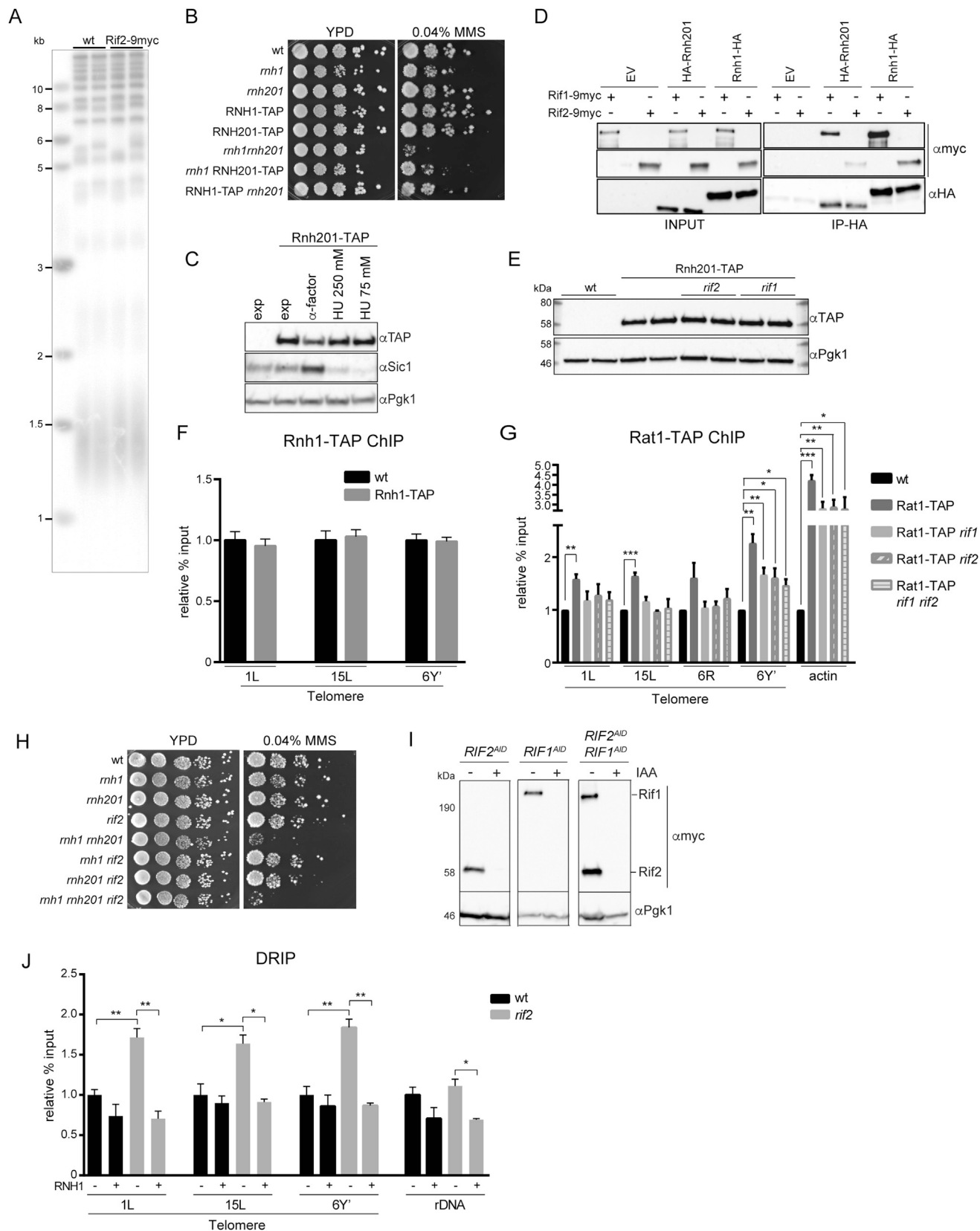   Telomere

(legend on next page)

Figure S4. Rif2 Recruits RNase H Activity to Telomeres, Related to Figure 4

(A) Southern blot analysis of bulk telomere length. DNA of the indicated strains was extracted and digested with XhoI. The blot was hybridized with a radioactive probe recognizing telomeric DNA. Rif2 dysfunction leads to drastic telomere elongation.

(B) Rnh1-TAP and Rnh201-TAP are functional. Serial dilutions of cells of the indicated genotypes were assayed on normal growth media (YPD) and media containing 0.04% MMS. Plates were imaged after 36 hr of incubation at 30°C.

(C) Cells endogenously expressing Rnh201-TAP were arrested with the indicated reagents and subjected to western blot to determine if Rnh201-TAP levels changed between HU 250 mM and HU 75 mM.

(D) Overexpressed Rnh1 and Rnh201 were precipitated in the presence of Rif1-9myc and Rif2-9myc and interactions were detected by western blotting as performed in Figure 4.

(E) Rnh201-TAP levels are not affected in *rif2* and *rif1* mutants. Protein levels were analyzed in the indicated genetic backgrounds by immunoblotting of protein extracts with PAP antibody (anti-Peroxidase anti-Peroxidase complex) and anti-phospho-glycerate kinase (PGK1) as loading control.

(F) Rnh1 does not localize to telomeres. ChIP of cross-linked samples was performed to determine the abundance of TAP-tagged Rnh1 at telomeres. The mean values + SEM are depicted. n = 3.

(G) Rat1 abundance at telomeres is influenced by Rif1 and Rif2. Cells of indicated genotypes were crosslinked and Rat1-TAP was pulled down from the extracts with IgG beads. Rat1-TAP enrichment was determined via qPCR. The mean values normalized to an untagged control + SEM are depicted. n = 3; *p < 0.05, **p < 0.01, ***p < 0.001.

(H) Rif2 is not required for Rnh201 genome-wide function. Serial dilution of cells of the indicated genotypes were assayed on normal growth media (YPD) and media containing 0.04% MMS. Plates were imaged after 24 hr of incubation at 30°C + 24 hr at room temperature.

(I) Rif1 and Rif2 protein levels were analyzed before and after IAA addition using anti-MYC antibodies. Pgk1 protein levels are shown as a loading control.

(J) *rif2* cells accumulate RNA-DNA hybrids. DRIP assay using the S9.6 antibody to measure RNA-DNA hybrid levels in cells of the indicated genotypes. RNH1+ indicates overexpression of *RNH1*. Values are represented as percentage input of DNA recovered relative to wild-type (WT), which is set to 1. Data are shown as mean + SEM of 3 biological replicates. p values were obtained from two-tailed Student's t tests. *p < 0.05, **p < 0.01.